Electronic Theses and Dissertations

Theses, Dissertations, and Major Papers

1975

ELECTRON SPIN RESONANCE STUDIES OF TRANSITION METAL COMPLEXES.

CHRISTOPHER CHIKE. EZZEH
University of Windsor

Follow this and additional works at: https://scholar.uwindsor.ca/etd

0

ELECTRON SPIN RESONANCE STUDIES

OF

TRANSITION METAL COMPLEXES

BY

CHRISTOPHER CHIKE EZZEH

A Dissertation

submitted to the Faculty of Graduate Studies

through the Department of Chemistry in

partial fulfillment of the requirements

for the degree of Doctor of Philosophy

at the University of Windsor

Windsor, Ontario

1975

578131

To

MARY ANN

and

my parents

OBI AND MRS. JOHNSON WALTER EZZEH

FOREWORD

The work described in this thesis was undertaken by the author in the Chemistry Department of the University of Windsor, Ontario, between 1972 and 1974.

Christopher Chike Ezzeh

Windsor, Ontario

January 1975

<center>ABSTRACT</center>

ELECTRON SPIN RESONANCE STUDIES OF TRANSITION METAL COMPLEXES

In order to determine the charge transfer in the

Mn-O bond the electron spin resonance study of the MnO_4^{2-} ion

in dilute single crystals of the orthorhombic host $BaSeO_4$ has

been done at $4°K$. The principal g and A values are $g_x = 1.9580$

±0.0004, $g_y = 1.9655\pm0.0008$, $g_z = 1.9824\pm0.0004$, $A_x=(126.0\pm0.4)$

$\times 10^{-4} cm^{-1}$, $A_y=(84.2\pm0.4)\times 10^{-4} cm^{-1}$ and $A_z=(16.3\pm0.4)\times 10^{-4}$

cm^{-1}. The x,y and z axes are chosen so that the y axis is along

the b crystallographic axis while the x and z axes are nine

degrees away from the c and a crystallographic axes respectively.

The principal x and z axes of the g and A values in the ac

plane are found to differ by $4°$. The ground state is shown to

be the d_{z^2} orbital with a 2% admixture of $d_{x^2-y^2}$ orbital,

similar to that of MnO_4^{2-} in $BaSO_4$ but different from that of

MnO_4^{2-} in K_2CrO_4 where the ground state was shown to be the

d_{xy} orbital. It is shown that for MnO_4^{2-} in $BaSeO_4$ the

difference in the principal x and z axes of the g and A

values is attributable to an admixture of the d_{yz} orbital

with the d_{xy} orbital which is estimated to be about 0.03%

from the angular separation of the axes. An MO analysis of the

ESR data for MnO_4^{2-} in $BaSeO_4$ and $BaSO_4$ shows that the d orbital

contribution to the molecular orbitals occupied by the unpaired

electron are close to those of a +2 charged free ion. A further

analysis shows the pattern of charge transfer in the Mn-O bond. There is more σ charge transfer and less π charge transfer when MnO_4^{2-} substitutes for the smaller SO_4^{2-} than when it substitutes for the larger SeO_4^{2-} ion.

Also the ESR of dilute single crystals of $Fe(CN)_5NH_3^{2-}$ ion in $Fe(CN)_5NO.2H_2O$ has been investigated at $4°K$. The principal g values are $g_x = 0.845 \pm 0.001$, $g_y = 2.177 \pm 0.001$ and $g_z = 2.995 \pm 0.001$. The hyperfine interaction for the amine nitrogen was observed and found to be $0 \leqslant A_x \leqslant +2.2 \times 10^{-4}$ cm^{-1}, $0 \geqslant A_y \geqslant -3.7 \times 10^{-4} cm^{-1}$ and $A_z = (+8.1 \pm 0.4) \times 10^{-4} cm^{-1}$. The g values are consistent only with a ground state in which the unpaired electron is primarily in a d_{xz} orbital rather than the expected $d_{x^2-y^2}$ orbital. The large anisotropy in the hyperfine interaction is explained as requiring a 20% transfer of electron spin to the amine nitrogen. This unusual ground state and covalency of the Fe-N bond suggest that NH_3 in this complex has a much stronger ligand field strength than is found in other complexes.

TABLE OF CONTENTS

LIST OF FIGURES

Chapter 1

INTRODUCTION

A. Scope of this work

The splitting of the d orbitals of metal ions by their environment has been a subject of interest to chemists. In octahedral and tetrahedral symmetries these orbitals are split into a group of three designated as t_2 and a pair designated as e. In an octahedral environment the e_g orbitals are higher in energy than the t_{2g} orbitals, while in a tetrahedral field the t_2 orbitals are higher in energy than the e orbitals. Distortions from either octahedral or tetrahedral symmetries further split the energies of each group of orbitals. An understanding of the crystal field theory is useful in order to predict the number of unpaired electrons that a transition metal ion possesses in various crystal fields and hence the actual magnetic moments. Electron spin resonance studies of paramagnetic ions provide useful information about the wave function describing the unpaired electrons both in the ground state and in the excited electronic states. This information is obtained from the spin hamiltonian parameters that are directly determined by the experimental measurements.

The study of the complexes mentioned below was undertaken to determine their spin Hamiltonian parameters, to analyze these parameters in order to determine the ground state of the metal ions, and to perform a molecular orbital analysis of these parameters in order to determine the charge transfer in the metal-ligand bonds. These ions have been

1

studied in single crystals diluted with an isomorphic dia-
magnetic host to reduce interactions between neighboring
paramagnetic ions. The principal ions studied in this work
are the manganate ion in barium selenate and the pentacyano-
ammine ferrate(III) ion in sodium nitroprusside. Manganese(VI)
has a d^1 configuration while iron(III) has a d^5 configuration.
The d^5 configuration in an octahedral crystal field can be
treated by the hole formalism so that it is similar to the
d^1 system.

B. Historical

Since the discovery of the technique by Zavoisky[1],
ESR has provided much information on inorganic systems. Among
the interesting systems studied are d^1 and d^5, which have been
studied in some detail recently. Manganese(VI) is a d^1 system
and its tetrahedral oxyanion has been studied in different
hosts. Carrington et al.[2] investigated the MnO_4^{2-} ion in
K_2CrO_4 host and their data were analysed by Schonland[3] who
found the unpaired electron to be in the d_{xy} orbital. The
CrO_4^{2-} ion in K_2CrO_4 has a site symmetry of C_s and the z axis
was chosen as the principal axis that lies in the symmetry
plane of the ion and comes closest to bisecting the angle
between the two oxygen atoms in the plane. The x and y axes
are perpendicular to this axis with one being in the plane
of symmetry and the other perpendicular to it. In this study
we have designated the y axis to be the one perpendicular
to the plane. Subsequent investigations of other d^1
tetrahedral oxyanions: MnO_4^{2-} in $BaSO_4$ by Kosky et al.[4]
CrO_4^{3-} in Ca_2PO_4Cl and $Ca_5(PO_4)_3Cl$ by Banks, Greenblatt

and McGarvey[5,6], and MoO_4^{3-} in $CaWO_4$ by Azerbayejani and Merlo[7] found the unpaired electron in the d_{z^2} orbital for these complexes. Ballhausen and Liehr[8] have proposed an energy level scheme for the manganate and hypochromate ions in which the unpaired electron occupied one of the e orbitals. Since the d_{z^2} orbital is one of the e orbitals, it is apparent that these ESR results demonstrate the correctness of this energy level scheme. The fact that the unpaired electron of MnO_4^{2-} ion in K_2CrO_4 and in $BaSO_4$ occupies different d orbitals is puzzling since both host lattices belong to the same space group, Pnma, and their oxyanion tetrahedra have similar bond angles as shown in Tables 1,7 and 11. Kosky et al.[4] suggested that the smaller size of SO_4^{2-} ion relative to the MnO_4^{2-} and CrO_4^{2-} ions might cause a different distortion for MnO_4^{2-} in $BaSO_4$. Since SeO_4^{2-} ion is likely to be more nearly the size of the MnO_4^{2-} ion, it was decided to study the MnO_4^{2-} ion in single crystals of $BaSeO_4$ to determine the effect that the lattice size has upon the distortion present in the MnO_4^{2-} ion.

A d^5 system in an octahedral environment can be analyzed mathematically using the hole formalism. The first reported paramagnetic resonance work on a d^5 system, $Fe(CN)_6^{3-}$, was by Baker, Bleaney and Bowers[9]. Bleaney and O'Brien[10] later developed the theory of the complex cyanides of the iron group. Since then a large number of d^5 $\{(t_{2g})^5\}$ complexes have been studied. Among the most recently reported studies are : Ru^{3+} in Yttrium Gallium garnet[11], Fe^{3+} complexes with sulfur-containing ligands [12], Fe(III) N,N-dimethyldithio-carbamate[13], Fe(phenanthroline)$_2$(CN)$_2^+$[14] and trisbidentate

complexes of Fe(III), Ru(III), Os(III) with sulfur donor ligands[15]. Most of these studies were done on frozen glasses or powders. Single crystal studies of the strong field d^5 complexes have been reported for $Fe(CN)_6^{3-}$ and $Mn(CN)_6^{4-[9]}$, $Ru(H_2O)_6^{3+[11]}$, $IrBr_6^{2-}$ and $IrCl_6^{2-[16]}$, $Ru(NH_3)_6^{3+[17]}$, $Ru(acac)_3^{[18]}$, $Os\{P(C_2H_5)_2C_6H_5\}_2^{[19]}$ and the formally d^5 complexes of $Mn(CN)_5NO^{2-[20,21]}$ and $Cr(CN)_5NO^{3-[20,22,23]}$. In many of these, the site symmetries are lowered as a result of geometric distortions such as inequivalent atom positions and this results in crystal field splittings of the t_{2g} orbitals of several hundred reciprocal centimeters. It thus appears that additional single crystal studies of iron complexes, such as $Fe(CN)_5NH_3^{2-}$, in which the major distortions from octahedral symmetry are attributable to a sixth inequivalent ligand in the first coordination sphere, would be valuable in interpreting the considerable data on powders and frozen glasses. This investigation would also provide some information about the wave functions for the three Kramers doublets that make up the $\{(t_{2g})^5\}$ configuration. This can be obtained from a low temperature study of the complex ion of interest.

C. Charge Transfer in Metal-Ligand Bonds

Charge transfer in metal-ligand bonds has been esti-mated using the molecular orbital parameters determined from ESR studies. For transition metal complexes, molecular orbital models have been found appropriate because they take account of the atomic orbitals belonging to the ligand atoms and therefore introduce covalency to the bonding. The importance

of covalent bonding in these complexes is supported by the short metal-oxygen bonds for oxyanions and cations, large reductions of the metal spin orbit coupling parameters and hyperfine interaction with ligand nuclei that have nuclear moments, which show that the unpaired electron is delocalized. Owen[24] and Stevens[25] were the first to use the molecular orbital theory to calculate the effects on the magnetogyric ratio of the electron arising from covalent bonding in Cu(II) and Ni(II) compounds. Some d^1 complexes for which the molecular orbital treatments have been given are: $CrOCl_n^{(n-3)-}$, n=4 and 5 by Kon et al.[26], $MoOCl_5^{2-}$, $VOCl_5^{3-}$ and $VO(H_2O)_5^{2-}$ by DeArmond et al.[27], $Ti(acac)_3$ by McGarvey[28] and $CrCl_5(H_2O)^{2-}$ by Garrett et al.[29] Most recently McGarvey[30] has performed a self consistent charge analysis on the ESR spin Hamiltonian parameters of CrO_4^{3-} and MoO_4^{3-}. In this analysis MO mixing coefficients are calculated from the spin Hamiltonian para- meters using excited state energies obtained from optical spectroscopy, values of the spin orbit coupling constant, ξ, for the d orbital obtained from atomic spectroscopy and values of $<r^{-3}>$ for the d orbital obtained from Hartree-Fock computations. The calculation is done for values of ξ and $<r^{-3}>$ appropriate to different charges on the free metal ion and a Mulliken charge analysis is done on the resulting molecular orbitals. The computation is deemed self-consistent when the Mulliken charge on the metal ion equals the charge associated with the values of ξ and $<r^{-3}>$ used. Such a method has been applied to determine the charge transfer in the Mn-O bond of the manganate ion in this study.

Chapter II

ELECTRON SPIN RESONANCE SPECTROMETER

Both the 300^OK and 77^OK electron spin resonance studies were done on a Varian E-12 spectrometer. The crystals investigated gave broad spectra at 77^OK and none at 300^OK because the spin lattice relaxation time, T_1, is short at these temperatures. Liquid helium temperature studies were done on a spectrometer built by Professor F. Holuj of the Physics Department of the University of Windsor. This was an X-band spectrometer. At low temperatures, the spin lattice relaxation time, T_1, is long, requiring the use of low powers. Measurements at low power makes it necessary to employ a superheterodyne system. Figure 1 shows a block diagram of the spectrometer used. 100 KHz field modulation was employed. A double Dewar system was used to hold the liquid helium. Liquid nitrogen was placed in the outer dewar while the inner dewar was evacuated to about 25 microns of mercury. This evacuation ensured a slow evaporation of the liquid helium.

A cylindrical cavity operating in the TE_{011} mode, shown in Figure 2, was used. A single crystal was mounted so that it could be rotated at 4^OK on a horizontal axis while the magnetic field could be rotated perpendicular to this axis. The crystal mount and gear system are also shown in Figure 2.

30MHz OSCILL.

LOC. OSC. POWER SUPPLY

30MHz AMP.

FREQ. STABIL.

LOC. OSCILL.

30MHz AMP. & DET.

P.S.D.

CHART RECORDER

30MHz I.F. STRIP

REF.

100KHz OSCILL.

12" MAGNET

MAGIC T

CIRCULATOR

PRECISION ATTENUATOR

CAVITY

60Hz MODULATION

KLYSTRON ISOLATOR

10 db COUPLER

KLYSTRON POWER SUPPLY

MONITOR

CRO

FREQ. STABIL.

10KHz OSCILL.

10KHz AMP.
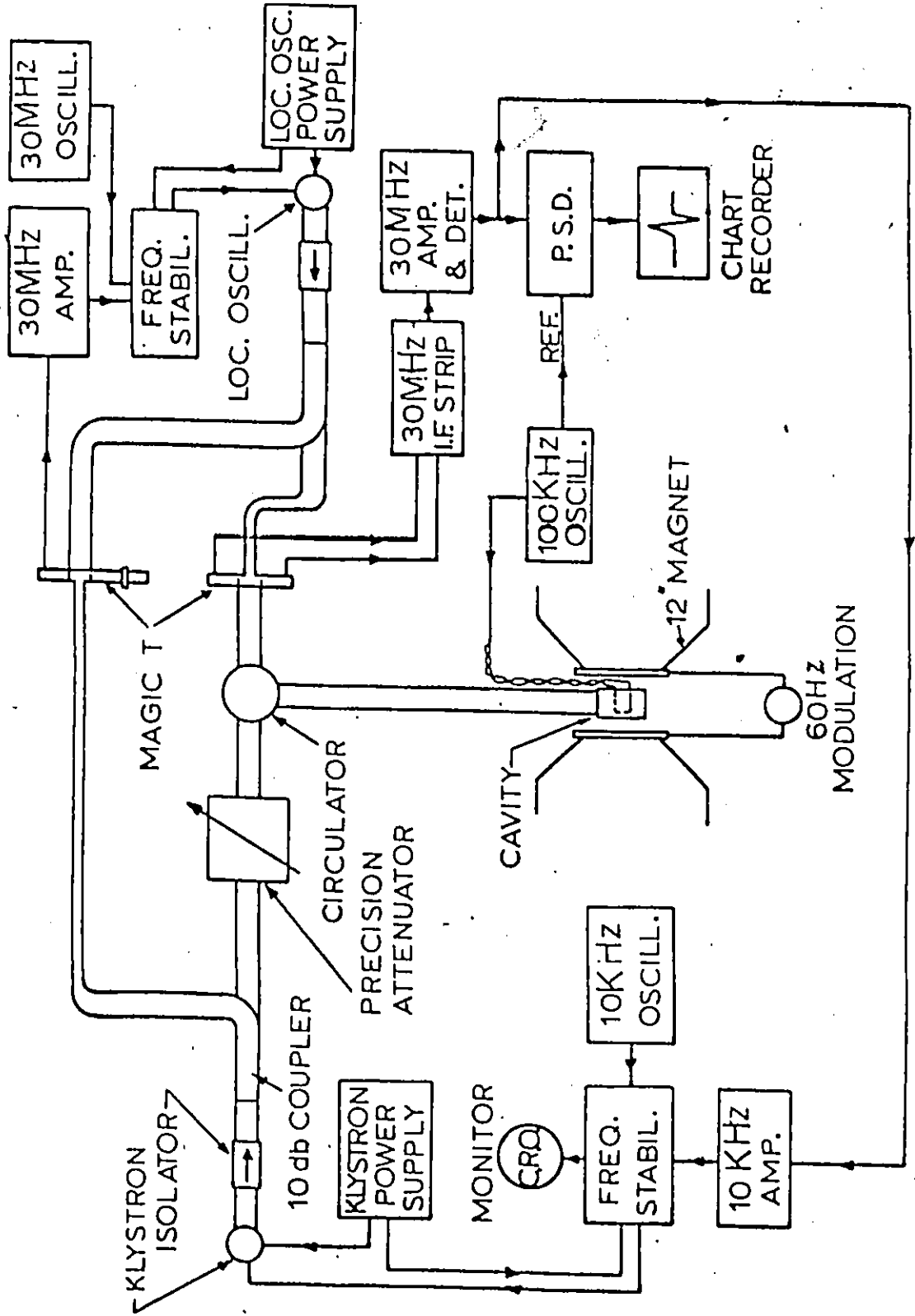
Figure 1. Block diagram of x-band superheterodyne spectrometer used for ESR experiments at liquid helium temperatures.
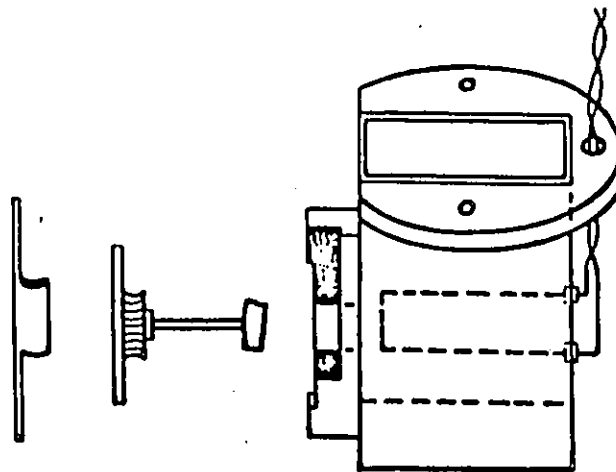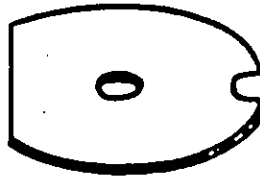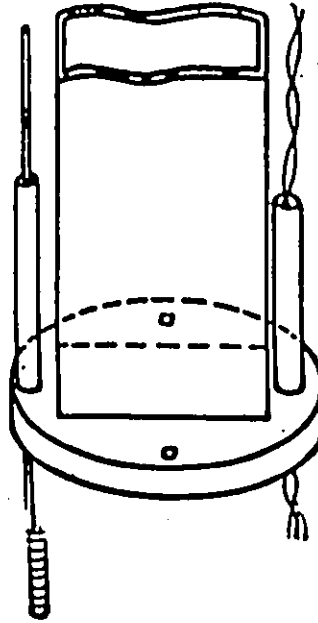
Figure 2. X-band cavity system with horizontal crystal mount.

Chapter III

CRYSTAL STRUCTURES

A. General Description:

The interpretation of ESR results in the solid state requires a knowledge of the crystal structure of the substance studied. In single crystal ESR studies the paramagnetic ion is introduced as an impurity into a diamagnetic and isomorphic host whose crystal structure is known. Since the paramagnetic ion substitutes for the diamagnetic ion in the lattice, it is generally assumed that the site symmetry for the paramagnetic ion is the same as for the diamagnetic ion.

The two diamagnetic hosts used in these studies are $BaSeO_4$ and $Na_2Fe(CN)_5NO \cdot 2H_2O$. Both are orthorhombic and have four molecules per unit cell. Each has a site symmetry of C_s at the metal ion. The four molecules in the unit cell are related pairwise by inversion centers as discussed below. The pairs are interchanged by a reflection in a plane containing the unique crystal axis and one parallel to the molecular plane.

B. Barium Selenate:

The complete crystal structure of $BaSeO_4$ has not been done but x-ray diffraction studies of powder samples[31,32] show it to be isomorphic with barium sulfate with similar unit cell dimensions. The unit cell constants for $BaSeO_4$, $BaSO_4$ and K_2CrO_4 are given in Table 1. $BaSeO_4$ crystals belong

TABLE 1

Space Group and Unit Cell Parameters

Space Group	$BaSO_4$ [33]	$BaSeO_4$ [32]	K_2CrO_4 [34]
Space Group	Pnma	Pnma	Pnma
a	8.87 $\overset{o}{A}$	8.98±0.02 $\overset{o}{A}$	7.61 $\overset{o}{A}$
b	5.45 $\overset{o}{A}$	5.66±0.03 $\overset{o}{A}$	10.40 $\overset{o}{A}$
c	7.15 $\overset{o}{A}$	7.35±0.01 $\overset{o}{A}$	5.92 $\overset{o}{A}$

to the orthorhombic space group Pnma, point symmetry mmm and have four molecules per unit cell. Each selenium atom is at the center of a distorted tetrahedron of four oxygen atoms, two of which lie in the ac plane which passes through the selenium nucleus. The other two are symmetrically situated above and below this plane with the line joining them parallel to the b axis. The site symmetry of each molecule is C_s.

In the space group Pnma, there is an inversion center at the point $0\frac{1}{2}0$. This inversion center relates the ion pair at the points $x\frac{1}{4}z$ and $\bar{x}(3/4)\bar{z}$ as well as those at $(\frac{1}{2}-x)3/4(\frac{1}{2}+z)$ and $(\frac{1}{2}+x)\frac{1}{4}(\frac{1}{2}-z)$. The two pairs are interchanged by a glide reflection across a plane parallel to the crystallographic ab plane. Thus in the mixed crystals, $Ba(Se,Mn)O_4$, there will be essentially two kinds of paramagnetic ions in the lattice, geometrically identical but distinguished by their differing orientations relative to the crystallographic axes.

C. Sodium Nitroprusside:

This crystal belongs to the space group Pnnm[35] with the lattice constants: $a = 11.8\text{Å}$, $b = 15.52\text{Å}$ and $c = 6.22\text{Å}$. In the nitroprusside ion, the plane of symmetry includes the Fe-N axis. Two equatorial cyanides are above and two are below this plane which is parallel to the ab plane of the crystal. The Fe-N-O systems are linear and make angles of $\pm33°$ with the crystallographic a axis. The equatorial cyanides are $90°$ apart so that there is no crystallographic reason to expect a major distortion of the crystal field from the axial symmetry.

In the substituted crystal, $Na_2Fe(CN)_5(NO,NH_3) \cdot 2H_2O$, the y_y

principal axis should be perpendicular to the ab plane. The$_y$

axis associated with the field parallel to the Fe - NH_3

direction should be about $\pm 33^{\circ}$ from the a axis.

In the $Na_2Fe(CN)_5NO \cdot 2H_2O$ the molecule centered about

the position xy0 and $\bar{x}\bar{y}0$ are related by inversion through the

origin so also is the pair at $(\frac{1}{2}-x)(\frac{1}{2}+y)\frac{1}{2}$ and $(\frac{1}{2}+x)(\frac{1}{2}-y)\frac{1}{2}$.

these two pairs are related by a glide reflection across either

a plane parallel to the crystallographic bc plane or one

parallel to the ac plane.

D. Identification of Crystal Axes:

$BaSO_4$ crystals grew prismatically elongated along the

[010] direction with (101) denoting the predominant faces. These

features were also expected for $BaSeO_4$. The long axis was

identified as the b axis for $BaSO_4$[4]. The same was assumed by

us for $BaSeO_4$ crystals. The a and c axes were roughly identified

by observing the interfacial angles.

Sodium Nitroprusside crystals are needle-like in

habit along the c axis. The predominant faces are (110). The

a and b axes were identified by visually considering the

interfacial angles.

Chapter IV

EXPERIMENTAL

A. Preparation of Single Crystals:

1. Preparation of $BaSeO_4$:

30g of Na_2SeO_4 were weighed out and dissolved in 600
ml of distilled water. To this solution were added 10 ml of 6N
HCl. The solution was then heated almost to boiling and 130 ml
of 0.5M $BaCl_2$ solution were added with stirring. The hot mixture
was further stirred for ten minutes, covered and allowed to
stand for 24 hours. The precipitate of $BaSeO_4$ was then filtered
through a sintered glass funnel, washed with hot water and
dried in an oven at $110^{\circ}C$.

2. Growth of Single Crystals of $Ba(Se,Mn)O_4$:

The first reported growth of single crystals of $BaSO_4$
and $Ba(S,Mn)O_4$ was by Wagner[36]. Patel and Koshy[37] subsequent-
ly grew single crystals of $BaSO_4$ by cooling a melt of an equi-
molar mixture of $BaCl_2$ and Na_2SO_4. In this study Wagner's
method was used. This method requires a platinum crucible since
the molten flux is caustic. A mixture containing 14% KCl, 30.8%
NaCl and 29.2% $BaSeO_4$ was thoroughly mixed at room temperature
and transferred to a platinum crucible. About 0.01g of $KMnO_4$
was added for each 25g of the starting material. The crucible
was placed in a temperature-controlled furnace which was
gradually heated to $780^{\circ}C$ in air. This temperature was chosen
after a few trial runs at various temperatures. Chloride ions
liberated at this temperature reduced the permanganate to the

13

manganate. The contents of the crucible were allowed to remain
at this temperature overnight and the furnace was cooled to
640°C at a rate of about 2.0 degrees per hour. The furnace was
then allowed to cool to room temperature without control. The
crystals were separated by dissolving the KCl-NaCl flux in hot
water. The crystals grew as small prisms about 6 mm long and
1 to 2 mm thick. The color of the substituted crystals varied
from pink to blue. The pink color is due to the presence of
permanganate. The ESR signals observed at 4°K indicated the
presence of manganate ions. No attempt was made to determine
the concentration of the manganate ion in the crystals.

3. Preparation of $Na_3Fe(CN)_5NH_3 \cdot 3H_2O$:

Sodium pentacyano ammino ferrate(III) was prepared
according to Brauer[38] by first preparing the diamagnetic
$Na_3Fe(CN)_5NH_3 \cdot 3H_2O$. 30g of sodium nitroprusside were weighed
out and dissolved along with 4g of NaOH in 120 ml of distilled
water. The mixture was cooled in an ice-water bath. At 0°C
ammonia was introduced until the solution was saturated
During the operation the temperature was not allowed to exceed
20°C. The solution was then kept under loose cover for several
hours at 0°C and the crystals which separated from the brownish
yellow solution were collected by filtration. The remainder
of the compound was precipitated from the solution by addition
of methanol. The product, $Na_3Fe(CN)_5NH_3 \cdot 3H_2O$, was purified by
solution in some cold water, from which it was precipitated
as fine yellow needles by careful addition of 90% alcohol. The
crystals were dried for several days in a vacuum desiccator

over calcium chloride.

4. **Oxidation of $Na_3Fe(CN)_5NH_3.3H_2O$ to $Na_2Fe(CN)_5NH_3.H_2O$:**

A solution of 20g of sodium nitrite in 50 ml of distilled water was treated at 0^OC with 20 ml of 30% acetic acid and then with 30g of $Na_3Fe(CN)_5NH_3.3H_2O$ prepared above. After two hours, a 1:1 mixture of alcohol and ether was added; this first precipitated a violet aquo complex salt (formed in a side reaction); further addition of alcohol-ether mixture precipitated the desired salt. This was purified by repeated solution in cold water and precipitation with alcohol. The dark yellow powder was dried to constant weight in vacuum over concentrated sulfuric acid.

5. **Growth of Single Crystals of $Na_2Fe(CN)_5(NO,NH_3).2H_2O$:**

To a saturated solution of sodium nitroprusside was added about 0.5% by weight of $Na_2Fe(CN)_5NH_3.H_2O$. The solution was thoroughly stirred and allowed to evaporate slowly over several days. The best crystals were obtained by evaporating ethanol-water solutions. The crystals grew as small prisms and varied in length and thickness. Well formed crystals 4 mm long and about 1 mm thick were used for ESR measurements.

B. Operational Techniques:

A well formed crystal of $BaSeO_4$ containing MnO_4^{2-} ion was selected for the study. This crystal was mounted by means of '5 Minute Epoxy' (manufactured by Le Page's Ltd., Montreal) to the end of a polyethylene rod with the b axis of the crystal approximately parallel to the axis of the rod. The polyethylene rod was attached to the cavity by means of the gear system shown in Figure 2. The magnet can be rotated about an axis orthogonal to that of the rod. Thus a combined rotation can align the b axis along the magnetic field direction. When the alignment of the axis is correct, the four molecules in the unit cell will be magnetically equivalent, thus giving identical resonances. A slight rotation of the magnet was found necessary to correctly align the b axis parallel to the magnetic field. This is at the intersection of two planes in which the resonances of the molecules in the crystal coincide. These are the ab and bc planes. Along the ab plane the g values show an increase as the magnetic field moves away from the b axis towards the a axis. The maximum g value occured when the magnetic field was along the a axis. 90° away from the a and b axis lies the c axis. The a and c axes were used to define the ac plane. Except when the magnetic field is along the a or c axis in the ac plane, the four molecules divide into two magnetically inequivalent pairs and the resonances of each pair are resolved. Spectra were recorded at selected points in the ac plane.

The same procedure was employed for $Fe(CN)_5NH_3^{2-}$ ion in $Na_2Fe(CN)_5NO \cdot 2H_2O$ crystal but the axes were differently labelled. The unique crystallographic axis was now the c axis.

Spectra were recorded at selected intervals in the ab plane.

The magnetic field of each ESR transition was determined by measuring the frequency of a proton resonance. The frequency of the proton oscillator was varied until the proton signal was observed on the oscilloscope. This frequency was measured with a Hewlett Packard No. 5253A Frequency counter. The value of the frequency so obtained was accurate to 1 kHz and since the magnetic field was homogeneous in this area it was not necessary to correct the value of the frequency for the probe position. The mechanical reproducibility of a given crystal setting was 0.5°.

THE SPIN HAMILTONIAN FOR d^1 IONS IN A
TETRAGONALLY DISTORTED ENVIRONMENT

A. <u>The General Hamiltonian:</u>

The energy of a transition metal ion in a crystal
field in the absence of an external magnetic field can be
described by a quantum mechanical Hamiltonian which includes
magnetic as well as electric interactions and can be written
as:

$$\mathcal{H} = \sum_i (p_i^2/2m) - \sum_i (Ze^2/r_i) + \sum_{i,j} e^2/r_{ij} + \sum_{i,j} \lambda_{ij} \underset{\sim}{\ell_i} \cdot \underset{\sim}{s_j}$$
$$\sum_i \underset{\sim}{s_i} \cdot \underset{\sim}{a_i} \cdot \underset{\sim}{I} - \sum_i e_i \varphi_c(r_i) + \mathcal{H}_{Quad.} \qquad (6)$$

in which $\Sigma(p_i^2/2m)$ is the total electron kinetic energy of
the paramagnetic ion, summed over each electron of the ion,
$\Sigma Ze^2/r_i$ is the coulomb attraction between the nucleus and
these electrons, $\Sigma e^2/r_{ij}$ is the coulomb repulsion between
electrons and is summed only over pairs of electrons,
$\Sigma \lambda_{ij} \underset{\sim}{\ell_i} \cdot \underset{\sim}{s_j}$ is the spin-orbit coupling with each i and j rang-
ing over all electrons, $\Sigma \underset{\sim}{s_i} \cdot \underset{\sim}{a_i} \cdot \underset{\sim}{I}$ is the magnetic interaction
between all electrons and the nucleus, $\Sigma e_i \phi_c(r_i)$ is the
crystal field interaction and $\mathcal{H}_{Quad.}$ is the nuclear
quadrupole interaction.

The first five terms represent the Hamiltonian for
the free ion. The fifth term is the crystal field inter-
action , a term in which it is assumed that crystal field
sources external to the ion give rise to electrostatic poten-
tial ϕ_c at the ion with which each electron interacts. The

symmetry of the crystal field determines the nature of·the

resulting energy levels and the extent of the degeneracy

remaining in them.

If the molecule is placed in a magnetic field H, two

additional terms must be added to the Hamiltonian given by

equation (6). These are:

$$\beta_e H \cdot (\underset{\sim}{L} + 2.0023 \underset{\sim}{S}) - g_N \beta_N \underset{\sim}{H} \cdot \underset{\sim}{I} \tag{7}$$

in which $\underset{\sim}{L}$ and $\underset{\sim}{S}$ are the orbital angular momentum and the

intrinsic spin vector operators respectively, β_N and β_e are

the nuclear and electronic magnetons respectively and g_N is

the nuclear g factor. $\underset{\sim}{I}$ is the nuclear spin vector operator.

These terms result from the interactions of the electronic

and the nuclear magnetic moments with the magnetic field.

B. The Spin Hamiltonian:

It is difficult to calculate the energy levels using

the above Hamiltonian but since in ESR one is concerned only

with the spin ·states of the electronic ground state, it is

possible to integrate out the electronic functional variables

and by second order perturbation theory derive a·spin Hamiltonian.

This Hamiltonian involves only spin operators, predicts the

ground state spin states and for $S = \frac{1}{2}$ for one nucleus, has

the form:

$$\mathcal{H}_S = \beta_e \underset{\sim}{H} \cdot \underset{\approx}{g} \cdot \underset{\sim}{S} + \underset{\sim}{I} \cdot \underset{\approx}{A} \cdot \underset{\sim}{S} \tag{8}$$

where $\underset{\sim}{H} \cdot \underset{\approx}{g} \cdot \underset{\sim}{S}$ is the magnetic Zeeman term in which $\underset{\sim}{H}$ is the

external magnetic field, $\underset{\sim}{S}$ is the electronic spin vector and

$\underset{\approx}{g}$ is a second order matrix. This term arises·from the inter-

action of the magnetic field with the spin and orbital angular

momenta of the electron. The second term $\underset{\sim}{I} \cdot \underset{\approx}{A} \cdot \underset{\sim}{S}$ is the hyperfine

splitting term in which $\underset{\sim}{I}$ and $\underset{\sim}{S}$ are the nuclear and electronic

spin magnetic momentum vectors respectively and $\underset{\infty}{A}$ is a second

order matrix. It can be shown that the hyperfine term can be

written as a sum of two terms, one representing the anisotropic

part which arises from the dipolar interaction between nuclear

and electronic spins which are not too close to each other,

and the other representing the isotropic part which arises

from the Fermi contact interaction due to the electron density

at the nucleus. The principal axes of the A and the g matrices

are usually oriented in the same or nearly the same direction.

These   axes can be conveniently determined by measuring the

ESR spectra of a single crystal.

Chapter VI

EXPERIMENTAL RESULTS

A. Manganate Ion in Barium Selenate:

1. The ESR Spectra:

The crystal structure of $Ba(Se,Mn)O_4$ predicts that
when the magnetic field is along the b axis of the crystal,
the magnitudes of the direction cosines for the magnetic field
relative to the molecular axes of all four molecules in the
unit cell are identical and only six lines will be expected.
These six lines are due to the hyperfine interaction of ^{55}Mn
nucleus which has a nuclear spin of 5/2 resulting in $(2I + 1)$
lines. The six lines were observed as expected and the spectrum
recorded in this orientation is shown in Figure 3. In the
crystallographic ac plane, the six lines should split into
two sets of six lines except when the magnetic field is along
either of the other two crystallographic axes. This splitting
of the six lines is caused by the fact that in this plane
the four molecules now divide into two magnetically inequi-
valent pairs. Twelve lines are therefore to be expected but in
general only eleven or ten lines were observed due to accidental
overlap of one or two lines. A typical spectrum recorded in the
ac plane is shown in Figure 4.

Since the molecular symmetry mirror plane coincides
with the crystallographic mirror plane, two principal axes of
$\underset{\approx}{g}$ must lie in the plane. The exact orientation of these with
respect to the crystallographic axes can be derived experimental-

21

22

103 GAUSS
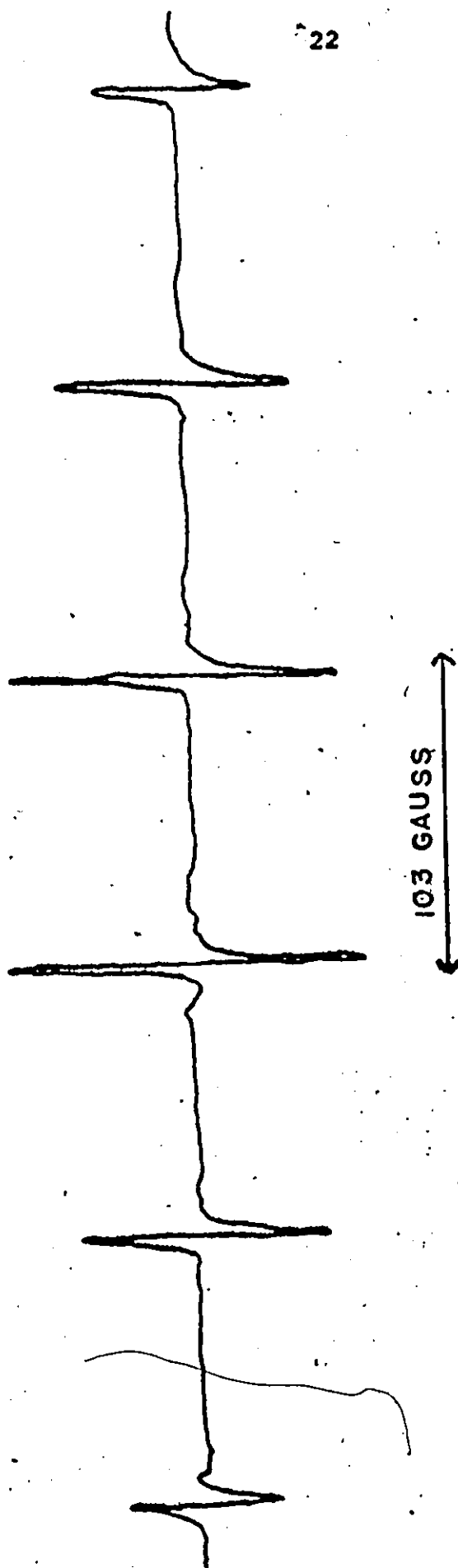
Figure 3. ESR Spectrum of MnO_4^{2-} in $BaSeO_4$ when the magnetic field

is along the b axis of the crystal.

23

189 GAUSS
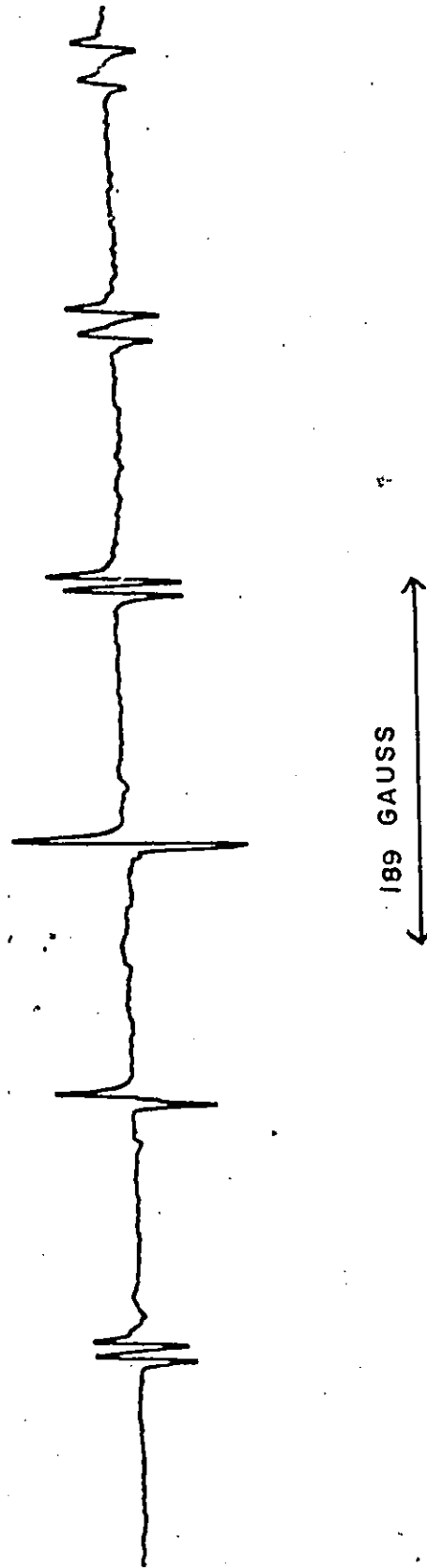
Figure 4. Typical ESR spectrum of MnO_4^{2-} in $BaSeO_4$ for rotation in the ac plane.

ly by plotting g^2 as a function of the angle of rotation in a specific plane. These two principal axes must be orthogonal and the third principal axis must be orthogonal to the mirror plane. This third principal axis, g_y is parallel to the b crystallographic axis. The positions of each resonance line of the spectra recorded in the ac plane are given in Table 2. The line width of the spectra are about one gauss and the line shape is nearly gaussian.

2.2. Determination of the Hyperfine Coupling Constant:

The angular dependence of g and A can be derived[39] by perturbation theory from the spin Hamiltonian given in equation (8). The first order results are given as :

$$h\nu(M_I) = g\beta H + KM_I \tag{9}$$

$$g = (g_x^2\cos^2\alpha + g_y^2\cos^2\beta + g_z^2\cos^2\gamma)^{1/2} \tag{10}$$

$$K = (g_x^2 A_x^2\cos^2\alpha + g_y^2 A_y^2\cos^2\beta + g_z^2 A_z^2\cos^2\gamma)^{1/2}/g \tag{11}$$

assuming g and A coaxial, where $\cos\alpha$, $\cos\beta$ and $\cos\gamma$ are the direction cosines between the principal axes and the magnetic field direction, g_x, g_y and g_z are the principal g values, A_x, A_y and A_z are the principal A values and M_I is the azimuthal magnetic quantum number for the nucleus.

Experimentally we vary H keeping ν constant. Solving equation (9) for H gives

$$H = (h\nu_0/g\beta) - (K/g\beta)M_I \tag{12}$$

where ν_0 is the frequency of the spectrometer and h is Planck's constant. Thus to first order, a spectrum of six equally spaced lines separated by $K/g\beta$ gauss and centered at

$h\nu_o/g\beta$ gauss is expected. When the hyperfine coupling is large

compared to $g\beta H$; equation (12) is no longer adequate and we

must include second order terms from perturbation solution

of equation (8). These terms are given in the Appendix.

Examination of these equations reveals that the

second order terms depend on M_I^2 only and therefore accurate

values of $K/g\beta$ can be obtained from the equation

$$-K/g\beta = \{H_{M_I} - H_{-M_I}\}/2|M_I| \tag{13}$$

Since there are three values of $|M_I|$, as given in Table 2,

we obtain three measurements of $K/g\beta$ from each spectrum using

equation (13). The average $K/g\beta$ values for different orient-

ations of the magnetic field in the ac plane are given in

Table 3 for each of the two resonances observed. Also the

value of $k/g\beta$ for the b axis is given.

The determination of K requires a value for g. Since

g need be known to only three or four significant figures for

this purpose, second order corrections are not necessary and

g was calculated from the value of the center field, $h\nu_o/g\beta$,

for the six line spectrum.

One of the principal axes must be along the b axis

and this has been designated the y axis. Therefore A_y is the

value of A found for the magnetic field along the crystallo-

graphic b axis. The x and z principal axes must be in the ac

plane and are found at the positions of the maximum and mini-

mum K values. For a rotation of the magnetic field in an

arbitrary crystal plane, equation (11) takes the form

$$g^2 K^2 = (gK)_{min}^2 + \{(gK)_{max}^2 - (gK)_{min}^2\}\cos^2(\theta - \theta_{max}) \tag{14}$$

TABLE 2

Resonance Positions in Gauss for Rotation in the ac Plane and Along the b-Axis

Angle	+5/2	+3/2	+1/2	-1/2	-3/2	-5/2

Line I

Angle	+5/2	+3/2	+1/2	-1/2	-3/2	-5/2
-9	3372.7	3381.6	3395.7	3413.6	3434.5	3459.4
0	3334.0	3368.1	3398.4	3426.7	3450.1	3479.6
9	3295.4	3348.2	3395.9	3442.2	3483.4	3523.7
20	3251.3	3323.6	3393.9	3462.2	2526.3	3587.4
35	3196.1	3293.2	3389.9	3486.1	3579.9	3672.9
50	3154.8	3272.3	3390.2	3509.6	3627.5	3744.9
65	3128.7	3258.3	3390.2	3522.4	3657.4	3792.2
81	3116.9	3252.5	3388.7	3526.7	3667.9	3808.4
97	3124.4	3263.7	3388.7	3520.3	3654.1	3787.4

Line II

Angle	+5/2	+3/2	+1/2	-1/2	-3/2	-5/2
-9	3295.4	3348.2	3395.9	3442.2	3483.4	3523.7
0	3334.0	3368.1	3398.4	3426.7	3450.1	3479.6
9	3372.7	3381.6	3395.7	3413.6	3434.5	3459.4
20	--	3369.4	3400.9	3430.5	3457.0	3486.4
35	3260.8	3327.1	3389.8	3452.0	3509.4	3564.3
50	3201.5	3295.3	3386.4	3477.2	3565.3	3650.0
65	3157.6	3271.4	3362.1	3499.0	3612.7	3724.7
81	3128.2	3257.6	3388.7	3518.3	3650.1	3780.9
97	3116.5	3263.7	3388.7	3526.7	3667.8	3807.7
b-Axis	3222.6	3308.8	3397.6	3489.4	3584.3	3680.6

TABLE 3

Hyperfine Splitting Constants, $K/g\beta$, in Gauss for Rotation

in the ac Plane for MnO_4^{2-} at 4 $^\circ K$

Angle	Line I	Line II
-9	17.6 ± 0.2	45.3 ± 0.5
0	28.2 ± 0.7	28.2 ± 0.7
9	45.3 ± 0.5	17.6 ± 0.2
20	67.6 ± 0.7	28.9 ± 0.7
35	95.8 ± 0.5	61.1 ± 0.7
50	118.1 ± 0.7	90.2 ± 0.7
65	132.7 ± 0.2	113.7 ± 0.2
81	137.9 ± 0.2	130.4 ± 0.2
97	132.2 ± 0.2	138.1 ± 0.2
b-axis	91.8 ± 0.2	

The angle is measured from the a axis.

where θ and θ_{max} are respectively the angles at which (gK) was measured at any specified orientation, and the angle at which (gK) is a maximum. $(gK)_{max}$ and $(gK)_{min}$ are the maximum and minimum values for (gK). The best values of $(gK)^2_{max}$, $(gK)^2_{min}$ and θ_{max} were found by fitting the values of K given in Table 3 to equation (14) with a least squares program written by Tepper[40] and slightly modified. The values of A_x, A_y and A_z and the angle α between the z principal axis of the hyperfine tensor and the a crystallographic axis are given in Table 4. Figure 5 shows a plot of K in gauss versus the angle θ in the ac plane. The z axis is chosen as the principal axis that lies in the symmetry plane of the ion and comes closest to bisecting the angle between the two oxygen atoms in the plane.

3. Determination of the g Values:

The appropriate values of g obtained by the first order equations must be corrected for second order terms. Using the estimated values of A_x, A_y, A_z, g_x, g_y and g_z the g values, for the various orientations, corrected for second order effects were calculated. The second order equations are not strictly valid in this case because, as will be seen later, the principal x and z axes are not the same for both the g and A tensors. However since the angle between the principal axes is small, the error incurred in using these equations is not more than the normal errors in determining line positions. Thus when the magnetic field is along the b axis of the crystal, the magnetic field H, for a specific value of M_I is given by :

$$H(M_I) = \frac{h\nu_o}{g_y\beta} - \frac{A_y}{g_y\beta}M_I - \frac{(A_z^2 + A_x^2)}{4g_y\beta h\nu_o}[I(I+1) - M_I^2] \quad (15a)$$

For two resonance lines of the same M_I, equation (15a) yields
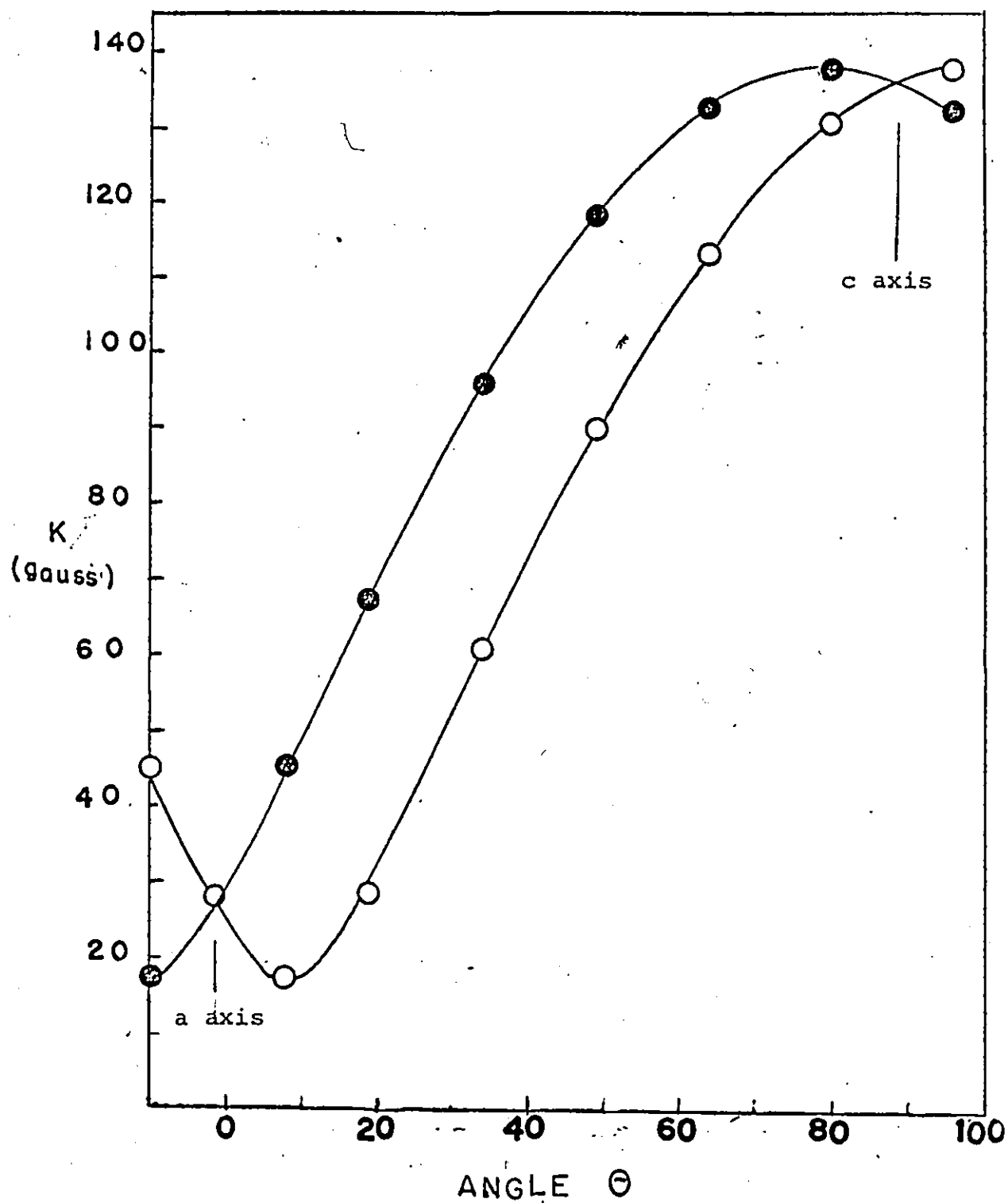
Figure 5. Plot of K in Gauss versus θ for MnO_4^{2-} in BaSeO$_4$ in the ac plane. θ is measured from the a axis.

TABLE 4

Principal g and A Values for MnO_4^{2-} at 4 °K

	$BaSeO_4$	$BaSO_4$[a]	K_2CrO_4[b]
g_x	1.9580 ± 0.0004	1.9600	1.966
g_y	1.9655 ± 0.0008	1.9687	1.970
g_z	1.9824 ± 0.0004	1.9800	1.938
$\alpha(g_z)$	13.4 ± 0.5°	13°	–
$A_x (10^{-4} \ cm^{-1})$	126.0 ± 0.4	128	33
$A_y (10^{-4} \ cm^{-1})$	84.2 ± 0.4	79	25
$A_z (10^{-4} \ cm^{-1})$	16.3 ± 0.4	48	135
$\alpha(A_z)$	9.2 ± 0.5°	13°	–

[a] Reference (4)

[b] Reference (2)

$$\frac{[H(M_I) + H(-M_I)]}{2} = H^O - \frac{(A_z^2 + A_x^2)}{4g_y\beta h\nu_o}[I(I + 1) - M_I^2] \qquad (15b)$$

where H^O is $(h\nu_o/g_y\beta_e)$ from which g_y is calculated.

Equation (15b) was solved for H^O and evaluated using the estimated values of A_z, A_x and g_y. Three values of H^O were obtained and their average used to calculate g_y corrected for second order effects.

For rotation in the ac plane the magnetic field $H(M_I)$ is given by:

$$H(M_I) = \frac{h\nu_o}{g\beta} - \frac{KM_I}{g\beta} - \frac{(A_z^2 A_x^2 + A_y^2 K^2)}{4g\beta K^2 h\nu_o}[I(I + 1) - M_I^2]$$

$$- \frac{g_x^2 g_z^2}{g^4}\frac{(A_x^2 - A_z^2)^2}{2K^2 g\beta h\nu_o} M_I^2 \sin^2\alpha \cos^2\alpha \qquad (16a)$$

where α is the angle between the z axis and the magnetic field, K ang g are the hyperfine splitting constant and g values respectively for a specific orientation in the ac plane. Again, for two resonance lines of the same M_I values, equation (16a) yields:

$$\frac{1}{2}[H(M_I) + H(-M_I)] = H^O - \frac{(A_z^2 A_x^2 + A_y^2 K^2)}{4g\beta h\nu_o K^2}[I(I + 1) - M_I^2]$$

$$- \frac{g_x^2 g_z^2}{g^4}\frac{(A_x^2 - A_z^2)^2}{2g\beta h\nu_o K^2}\sin^2\alpha\cos^2\alpha \cdot M_I^2 \qquad , \qquad (16b)$$

The last two terms of equation (16b) were estimated from the values of A_x, A_y, A_z, g_x, g_y, g_z and the angle α estimated from a plot of first order g^2 versus the angle θ defined above. Three values of H^O were obtained for a given orientation and their average was used to calculate the g values corrected for second order effects using equation (17)

$$g = (2.0036 \times H_{DPPH})/H^{o} \tag{17}$$

The values of H^{o}, g, and g^2 so obtained are given in Table 5.

For a rotation of the magnetic field in an arbitrary crystal plane, equation (10) takes the form:

$$g' = \{g_{min}^2 + (g_{max}^2 - g_{min}^2) \cos^2(\theta' - \theta_{max})\}^{\frac{1}{2}} \tag{18}$$

Using the computer program mentioned earlier the g values given in Table 5 were fitted to equation (18). The principal g values obtained have been given in Table 4. Figure 6 shows the plot of g^2 versus the angle θ in the ac plane for the experimental and computer-fitted curves. Table 6 gives the values of g^2K^2 in cm^{-2} used for the plot of g^2K^2 versus the angle θ in the ac plane shown in Figure 7.

Single crystal ESR studies of MnO_4^{2-} ion have been reported by Carrington et al.[2] in a K_2CrO_4 host lattice and by Kosky et al.[4] in a $BaSO_4$ host lattice. The principal g and A values in these two host lattices have been given in Table 4 for comparison with the corresponding values for the $BaSeO_4$ host lattice. The space group and unit cell parameters for these three hosts have been given in Table 1. Figure 8a shows one of the chromate tetrahedra projected onto (100) and Figure 8b shows one of the sulfate tetrahedra projected onto (010). It is assumed that since $BaSO_4$ and $BaSeO_4$ are iso-morphic Figure 8b will apply to $BaSeO_4$. The bond angles and the bond distances for all three ions are listed in Table 7. O_I and O_{II} are the two oxygen atoms in the molecular symmetry plane and O_{III} for SO_4^{2-} and CrO_4^{2-} represent the two oxygen atoms above and below this plane. For SeO_4^{2-}, space group Pmmm,
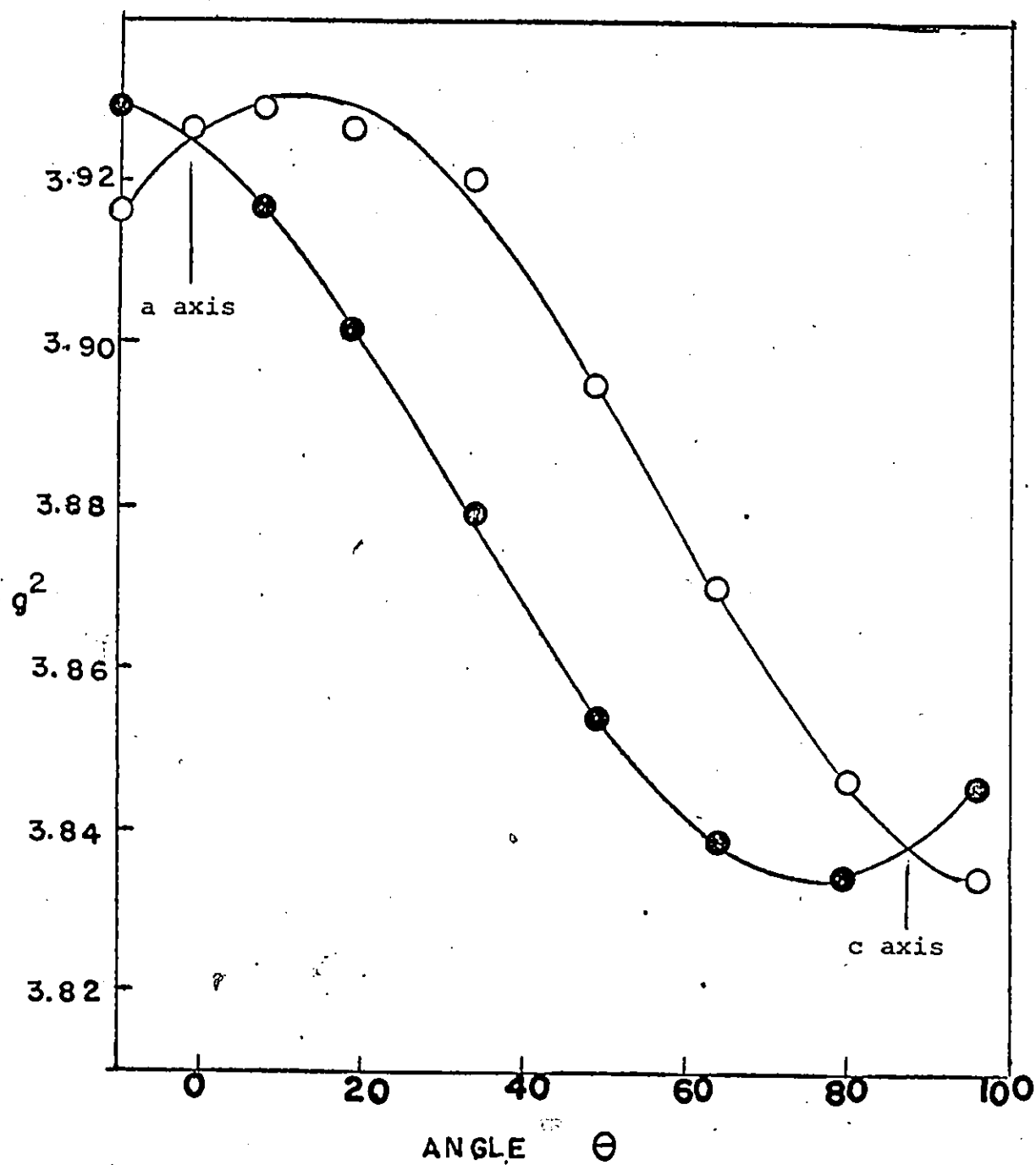
Figure 6. Plot of g^2 versus θ for MnO_4^{2-} in $BaSeO_4$ in the ac plane. θ is measured from the a axis.

TABLE 5

The Values H^O in Gauss and the Corresponding g and g^2

Values for Fotation in the ac Plane at 4 ^OK

at a Frequency of 9.425 GHz

Angle	H^O	g	g^2
		Line I	
-9	3422.5 ± 0.7	1.9822 ± 0.0004	3.9289
0	3423 ± 3	1.982 ± 0.002	3.9283
9	3427.9 ± 0.9	1.9790 ± 0.0005	3.9165
20	3434.5 ± 0.1	1.9752 ± 0.0001	3.9016
35	3444.1 ± 0.2	1.9697 ± 0.0001	3.8798
50	3455.6 ± 0.2	1.9632 ± 0.0001	3.8540
65	3462.4 ± 0.5	1.9593 ± 0.0003	3.8388
81	3464.3 ± 0.2	1.9582 ± 0.0001	3.8347
97	3459.4 ± 0.2	1.9610 ± 0.0001	3.8456
		Line II	
-9	3427.9 ± 0.9	1.9790 ± 0.0005	3.9165
0	3423 ± 3	1.982 ± 0.002	3.9283
9	3422.5 ± 0.7	1.9822 ± 0.0004	3.9289
20	3424 ± 2	1.9815 ± 0.0009	3.9262
35	3426 ± 1	1.9801 ± 0.0007	3.9208
50	3437.3 ± 0.7	1.9736 ± 0.0004	3.8952
65	3448.3 ± 0.2	1.9673 ± 0.0001	3.8703
81	3458.9 ± 0.2	1.9613 ± 0.0001	3.8467
97	3464.3 ± 0.9	1.9582 ± 0.0005	3.8347

Table 6

Values of g^2K^2 for MnO_4^{2-} in $BaSeO_4$ for the rotation in the
ac plane and at a Frequency of 9.425 GHz

Angle	$g^2K^2 \times 10^{-4}$ cm^{-1}	
	Line I	Line II
-9	0.104	0.687
0	0.267	0.267
9	0.687	0.104
20	1.618	0.280
35	3.016	1.249
50	4.518	2.690
65	5.656	4.219
81	6.092	5.480
97	5.636	6.113

The angle is measured from the a axis.
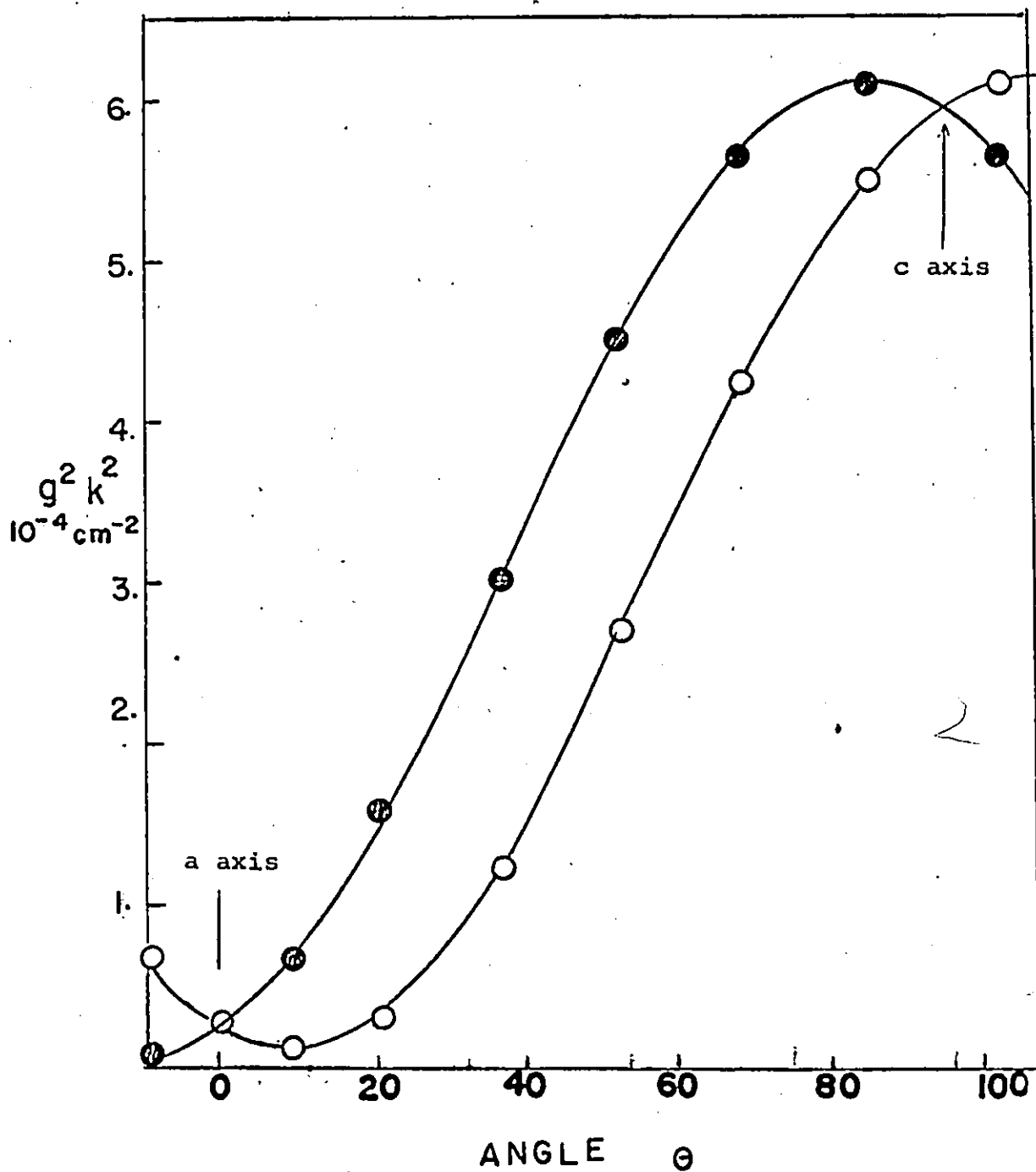
Figure 7. Plot of g^2K^2 versus θ for MnO_4^{2-} in $BaSeO_4$ in
the ac plane. θ is measured from the
a axis.

Figure 8. The principal g axes in the symmetry plane, for MnO_4^{2-} in (a) K_2CrO_4 and (b) $BaSO_4$
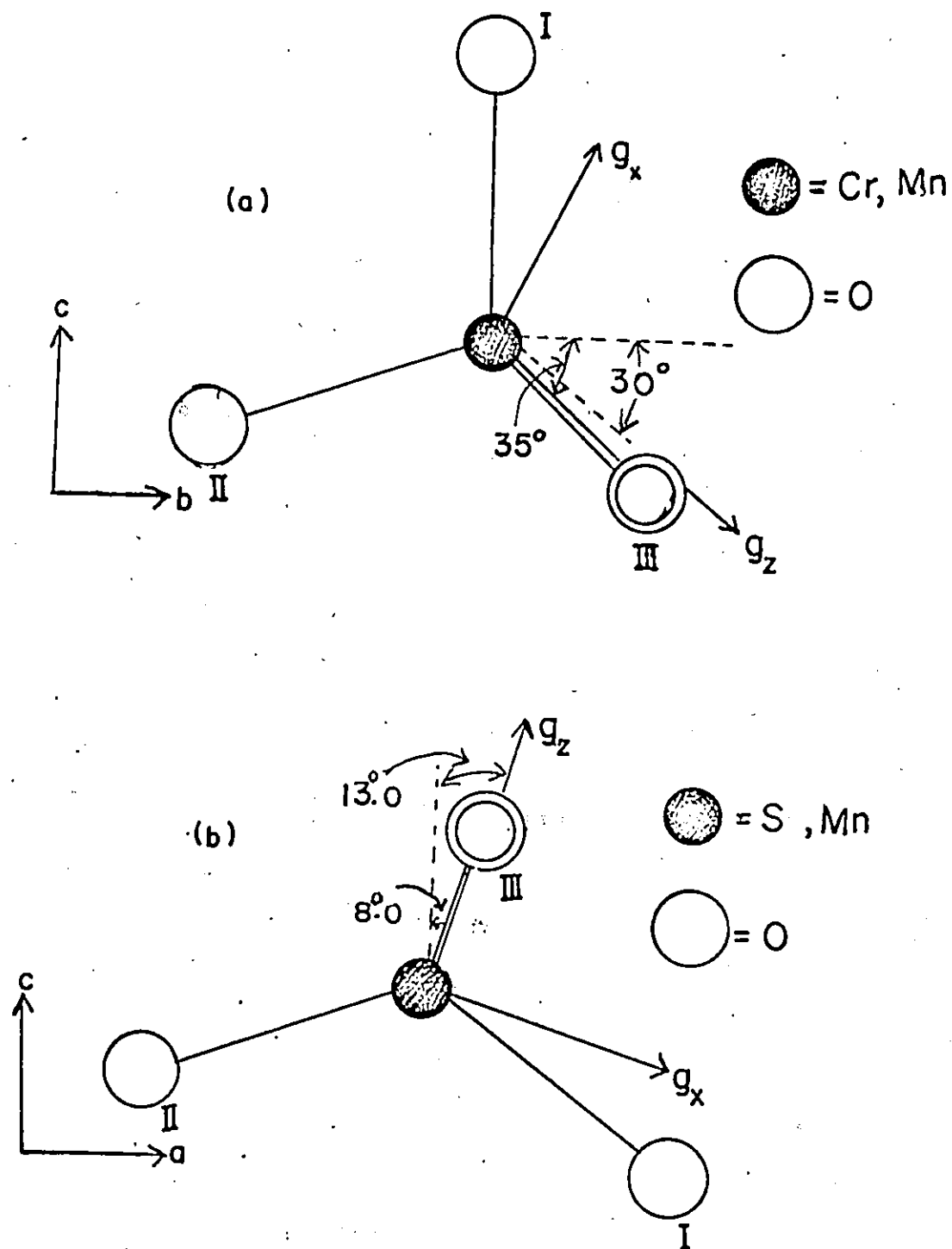
TABLE 7

Bond Angles and Bond Distances for SO_4^{2-}, SeO_4^{2-} and CrO_4^{2-} Tetrahedra

Bond Angles		Bond Distances	
SO_4^{2-}			
$O_{III} - S - O_{III}$	106°	$S - O_{III}$	1.48 Å
$O_{III} - S - O_I$	108°	$S - O_I$	1.50 Å
$O_I - S - O_{II}$	114°	$S - O_{II}$	1.52 Å
$O_{II} - S - O_{III}$	111°		
SeO_4^{2-} (a)			
$O_I - Se - O_{II}$	116°	$Se - O_I$	1.57 Å
$O_I - Se - O_{III}$	109°	$Se - O_{II}$	1.57 Å
$O_I - Se - O_{IV}$	112°	$Se - O_{III}$	1.64 Å
$O_{II} - Se - O_{III}$	112°	$Se - O_{IV}$	1.66 Å
$O_{II} - Se - O_{IV}$	106°		
$O_{III} - Se - O_{IV}$	106°		
CrO_4^{2-}			
$O_{III} - Cr - O_{III}$	105°	$Cr - O_{III}$	1.65 Å
$O_{III} - Cr - O_I$	109°	$Cr - O_I$	1.60 Å
$O_I - Cr - O_{II}$	111°	$Cr - O_{II}$	1.50 Å
$O_{II} - Cr - O_{III}$	112°		

(a) Bond angles and distances for SeO_4^{2-} were taken from reference 41 for H_2SeO_4.

O_{III} and O_{IV} are the counterparts of O_{III} but they are not identical to each other since they have different bond distances and angles. The site symmetry for CrO_4^{2-} and SO_4^{2-} is C_s. The principal g value directions for MnO_4^{2-} ion in K_2CrO_4 have been shown in figure 8a while those for MnO_4^{2-} ion in $BaSO_4$ are shown in Figure 8b. Both the g_z and g_x principal axes lie in the bc plane with the g_z axis displaced 5° from a line bisecting the O_{III} -Cr-O_{III} bond angle. The g_y principal axis direction is parallel to the a crystallographic axis. The g_z values for MnO_4^{2-} in both $BaSO_4$ and $BaSeO_4$ are the maximum values while the g_z value for MnO_4^{2-} in K_2CrO_4 is the minimum value. However, it has been found in $BaSeO_4$ that the maximum g value and the minimum hyperfine constant are directed 4° away from each other. This indicates that in the ac plane the principal axes of the g and A values are not the same. This has also been observed for MnO_4^{2-} in K_2CrO_4. The maximum value of the hyperfine splitting constant is along the z direction for MnO_4^{2-} in K_2CrO_4 while the minimum value is along the z direction for both $BaSO_4$ and $BaSeO_4$ hosts. Thus, as for the g values, the maxima and minima for the hyperfine splitting constants are reversed.

4. Forbidden Transitions:

When the magnetic field is along the a axis, some of the 'forbidden transitions', $\Delta M_S = 1$; $\Delta M_I = 1$, which were less intense in other orientations, now become more intense than normal transitions. The small value of the hyperfine splitting constant relative to the quadrupole interaction gave rise to these large quadrupole induced transitions.

However, the large overlap of the two resonances (forbidden and allowed) in this region precluded a careful orientation study thus making it difficult to obtain the values for the quadrupole terms in the spin Hamiltonian.

B. Amminopentacyanoferrate (III) ION in Sodium Nitroprusside:

1. The ESR Spectra:

The crystal structure of the host, sodium nitro-prusside, predicts that if $Fe(CN)_5NH_3^{2-}$ ion is substituted as expected, the four molecules in the unit cell will be magneti-cally equivalent when the magnetic field is along the unique crystallographic axis and thus will give rise to a single resonance signal. This unique crystallographic axis is the c axis and the ESR spectrum recorded when it is along the mag-netic field is shown in Figure 9. The line width of this spectrum is 6 gauss. In the crystallographic ab plane this single resonance splits into two lines since the four molecules in the unit cell now occur as two magnetically equivalent pairs. For all orientations in this plane, except when either of the two crystallographic axes are along the magnetic field, two lines were observed. Iron-57 has a nuclear spin of 1/2 but its abunbance is too small to give any observable hyperfine splitting. The only hyperfine splitting observed is that due to ^{14}N of the NH_3 group which is resolvable only when the magnetic field is near the z principal direction. The spectrum recorded when the magnetic field is along this direction is shown in Figure 10. The splitting was too small to be observed

10 GAUSS
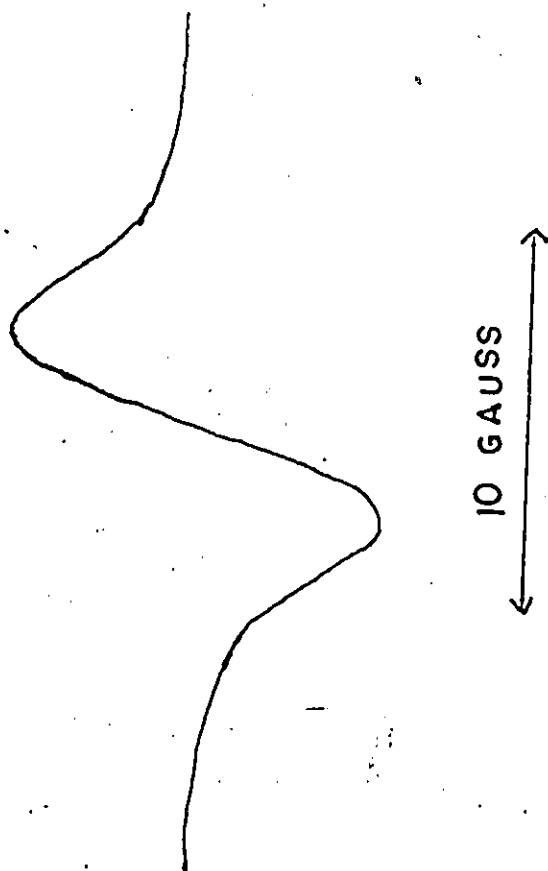
Figure 9. ESR spectrum of $Fe(CN)_5NH_3^{2-}$ in $Na_2Fe(CN)_5NO \cdot 2H_2O$ when the magnetic field is along the c axis of the crystal
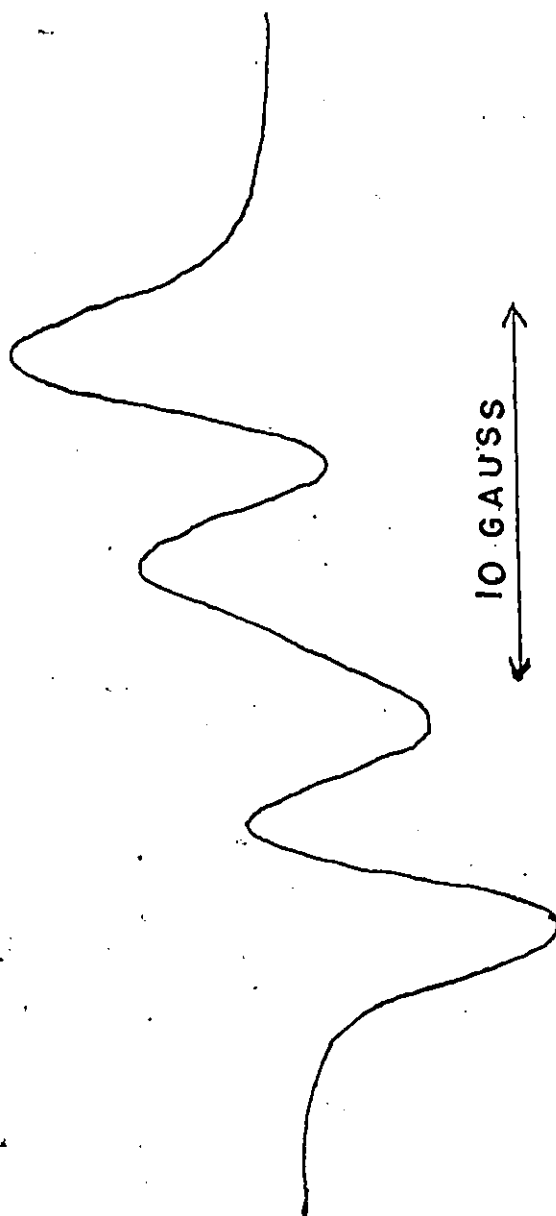
Figure 10. The ESR spectrum of Fe(CN)$_5$NH$_3^{2-}$ in Na$_2$Fe(CN)$_5$NO.2H$_2$O when the magnetic field is along the Fe-NH$_3$ bond axis

in the other two principal directions of g. In addition to these lines, some weak sharp lines were observed in some orientations. These weak lines were attributed to a strong field d^5 iron species by reason of the large variaiton in the g values with orientation. These may result from $Fe(CN)_5NH_3^{2-}$ ion doping into the site such that the NH_3 group occupies the position of a CN group instead of the preferred NO site. It was not possible to analyze these weak lines well enough to characterize their principal g values.

2. Determination of the g Values:

The angular dependence of the g value has been given in equation (10). Since two resonance lines were observed for the two pairs of magnetically inequivalent molecules during the rotation in the ab plane, the magnetic field of each line was determined by measuring the frequency of the proton nuclear magnetic resonance. Six reliable values were obtained for one line and four values for the other line and with a knowledge of the point of intersection of these lines, these values were combined for the g analysis. The values of these magnetic fields used in the combined g analysis are given in Table 8. Since DPPH (diphenylpicrylhydrazyl) was used as a reference, the g values were calculated from equation (17). Using the computer program mentioned earlier the experimental g values were fitted to equation (18). The plots of the g ang g^2 against the angle θ, defined with respect to the z axis, are shown in Figures 11 and 12 respectively.

As expected, both the ESR lines coincided in the c direction, which will be called the y direction in the complex.

Table 8

H in Gauss and g Values used for the Combined g analysis

for $Fe(CN)_5NH_3^{2-}$ in the ab Plane

Spectrometer Frequency 9.489 GHz

Angle	H(in Gauss)	g
0	2263 ± .5	2.9959 ±.001
15	2336.4 ±2	2.9018 ±.002
30	2580.5 ±5	2.6273 ±.005
44	3017.8 ±8	2.2465 ±.006
45	3062.5 ±12	2.2138 ±.008
59	4025.9 ±10	1.6840 ±.004
60	4036.7 ±21	1.6795 ±.008
75	6040.2 ±19	1.1224 ±.004
89	8004.3 ±20	0.8470 ±.002
104	6258.3 ±12	1.0833 ±.002

The angle is measured from the z principal axis.
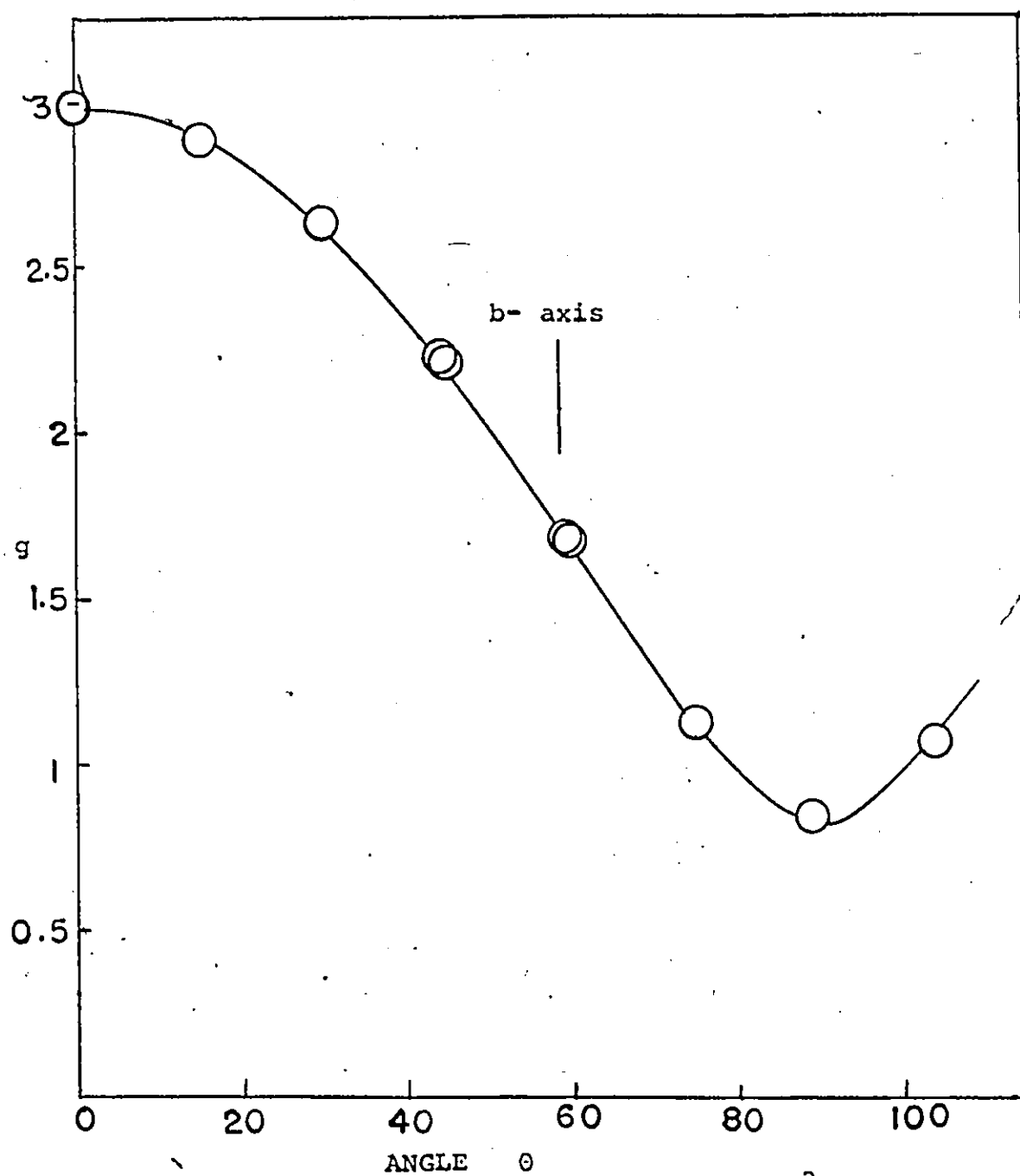
Figure 11. Plot of g versus θ for $Fe(CN)_5NH_3^{2-}$ ion in

$Na_2Fe(CN)_5NO.2H_2O$ for rotation in the ab plane
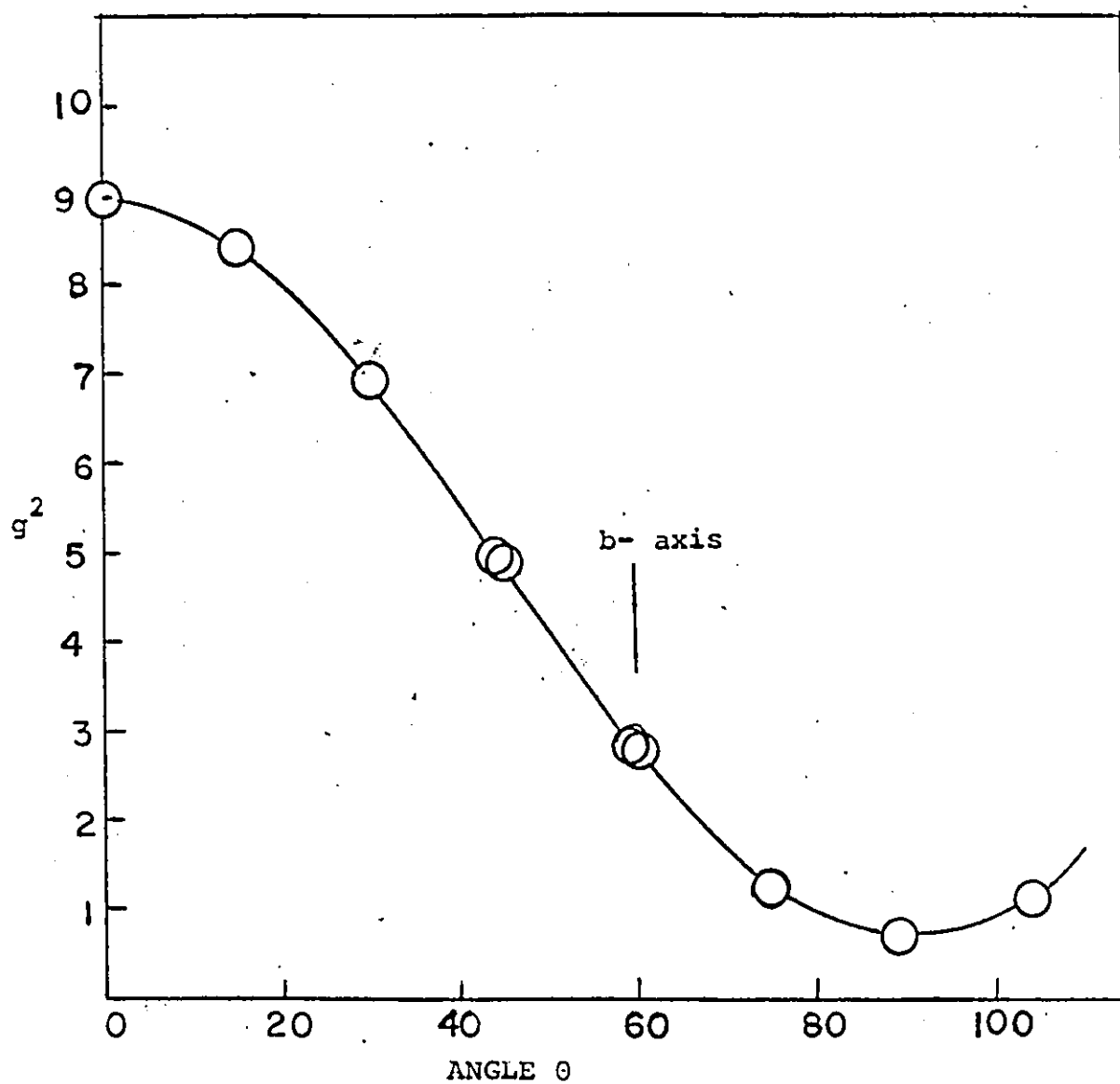
Figure 12. Plot of g^2 versus θ for $Fe(CN)_5NH_3^{2-}$ ion in $Na_2Fe(CN)_5NO.2H_2O$ for rotation in the ab plane

The two other principal directions are in the ab plane making angles of $\pm 31°$ and $\mp 59°$ to the a axis. The principal axis at $31°$ will be called the z direction and is associated with the $Fe - NH_3$ direction in the complex ion. The other principal axis in this plane at $-59°$ will be called the x direction.

3. Nitrogen Hyperfine Splitting:

When the magnetic field is near the z principal axis three hyperfine lines are observed. Nitrogen-14 has a nuclear spin $I = 1$. This splits the single resonance of iron into three components. The three lines were measured with proton NMR and the central line was used to calculate the g value. The hyperfine splitting constant was determined by taking the average of the differences between the two outer lines and the central line. This was found to have a value of 5.8 gauss. Attempts to obtain the extrapolated values of the hyperfine splitting in the other principal directions by plotting g^2K^2 versus $\cos^2\theta$ were unsuccessful because both g^2 and K^2 decreased rapidly making extrapolation uncertain. In these directions the line widths were used to estimate an upper limit on the magnitude of the hyperfine interaction by taking one half of the line width. These values as well as the principal g values and the orientation of the z and x principal axes with respect to the a axis are given in Table 9.

TABLE 9

Principal g and A Values for $Fe(CN)_5NH_3^{2-}$ at 4 $^\circ K$

$$g_x = 0.8470 \pm .002$$

$$g_y = 2.177 \pm 0.001$$

$$g_z = 2.9959 \pm .001$$

$$|A_x| \leq 2.2 \times 10^{-4} \text{ cm}^{-1}$$

$$|A_y| \leq 3.7 \times 10^{-4} \text{ cm}^{-1}$$

$$A_z = 8.1 \pm 0.4 \times 10^{-4} \text{ cm}^{-1}$$

$$\theta_z = 31^\circ$$

$$\theta_x = 59^\circ$$

where θ_z and θ_x are the angles between the z and x axes and the a axis of the crystal respectively.

Chapter VII

ANALYSIS OF THE SPIN HAMILTONIAN PARAMETERS

Two approaches have been used in the analysis of the spin Hamiltonian parameters. These are the Crystal Field Theory and the Molecular Orbital Theory. The Crystal Field Theory treats the interaction between the metal ion and the ligand as purely electrostatic, the ligand atoms or ions being represented as point charges. It does not take into account the partly covalent nature of the metal-ligand bonds. On the other hand, the Molecualr Orbital Theory takes into account the metal-ligand interaction which it describes in terms of molecular orbitals formed by the overlap of ligand and metal orbitals. The use of these two methods in the analysis of the spin Hamiltonian is discussed below.

A. The Crystal Field Approach to the Analysis of the Spin Hamiltonian Parameters for MnO_4^{2-} in $BaSeO_4$:

This theory predicts a splitting of the d orbital levels in a tetrahedral molecule such that the orbitals belonging to the E irreducible representation lie lower in energy than the T_2 irreducible representation. The single d electron may be either in the d_{z^2} or d_{xy} orbital. The axes are chosen so that the z axis is an improper rotation axis for the D_{2d} symmetry while the x and y axes are in the mirror planes. A comparison of the spin Hamiltonian parameters for MnO_4^{2-} in both $BaSO_4$ and $BaSeO_4$ listed in Table 4 shows that they are similar.

49

Kosky et al.[4] have analyzed the spin Hamiltonian parameters for MnO_4^{2-} in $BaSO_4$ considering the two possible ground states of d_z2 and d_{xy} orbitals. Their results show that while physically meaningful parameters were obtained assuming d_z2 ground state, no physically reasonable parameters were obtained assuming d_{xy} as the ground state. Thus their analysis favors the d_z2 ground state for MnO_4^{2-} in both $BaSO_4$ and $BaSeO_4$. In this study it was found that the linewidths of the ESR spectra are narrower than those found in the studies of Kosky et al.[4] and Banks et al.[5] These narrower lines resulted in greater accuracy in the determination of g and A values and hence, to the finding that their principal axes are not the same. This requires us to assume no higher a local symmetry than the site symmetry C_s. In this symmetry group the d_z2, d_{x2-y2} and the d_{xz} orbitals belong to the same irreducible representation if the symmetry plane is taken to be in the xz plane. The d_{xy} orbital must lie close in energy to the d_z2 orbital since liquid helium temperatures were required to observe a resonance signal, indicating a short spin-lattice relaxation time, T_1. The general d orbitals can be written as:

$$\psi_z2 = ad_z2 + bd_{x2-y2} + cd_{xz}$$

$$\psi_{x2-y2} = a_1 d_{x2-y2} + b_1 d_z2 + c_1 d_{xz}$$

$$\psi_{xz} = a_2 d_{xz} + b_2 d_{x2-y2} + c_2 d_z2 \qquad (20)$$

$$\psi_{xy} = e d_{xy} + f d_{yz}$$

$$\psi_{yz} = e d_{yz} + f d_{xy}$$

Normalization and orthogonalization require that

$$ab_1 + ba_1 + cc_1 = 0;$$

$$ac_2 + bb_2 + ca_2 = 0;$$

$$a_1b_2 + b_1c_2 + c_1a_2 = 0;$$

$$a_1a_2 + b_1b_2 + c_1c_2 = 1;$$

$$e^2 + f^2 = 1.$$

If the ground state is ψ_z2, perturbation method can be used to estimate the effects of the spin-orbit terms since the mixing of the closest state, ψ_{xy}, by spin-orbit coupling gives terms of small magnitude. The resulting two Kramers doublets were obtained by McGarvey[42] and are given by:

$$\psi_+ = \psi_{z2}^+ - iA\psi_{xy}^+ - iB\psi_{yz}^+ - (1/2)C\psi_{x2-y2}^- + (1/2)D\psi_{xz}^-$$

$$+ (i/2)E\psi_{xy}^- + (i/2)F\psi_{yz}^-;$$

$$(20)$$

$$\psi_- = \psi_{z2}^- + iA\psi_{xy}^- + iB\psi_{yz}^- + (1/2)C\psi_{x2-y2}^+ - (1/2)D\psi_{xz}^+$$

$$+ (i/2)E\psi_{xy}^+ + (i/2)F\psi_{yz}^+$$

where ψ_+ and ψ_- are spin up and spin down wave functions,

$$A = \left(\frac{2be + cf}{2}\right) \frac{\xi}{\Delta E_{xy}};$$

$$B = \left(\frac{ce - 2bf}{2}\right) \frac{\xi}{\Delta E_{yz}};$$

$$C = [c(\sqrt{3}b_1 - a_1) - c_1(\sqrt{3}a - b)]\xi/\Delta E_{x2-y2};$$

$$D = [e(\sqrt{3}a + b - fc)]\xi/\Delta E_{xz};$$

$$E = [f(\sqrt{3}a + b) + ec]\xi/\Delta E_{yz};$$

$$F = [e(\sqrt{3}a + b) - fc]\xi/\Delta E_{yz}$$

and ξ is the spin orbit coupling constant. ΔE_{yz}, ΔE_{xy}, ΔE_{xz} and ΔE_{x2-y2} are the energy differences between the ground

state ψ_{z^2} and the states ψ_{yz}, ψ_{xy}, ψ_{xz} and $\psi_{x^2-y^2}$.

The actual values of the coefficients in equation (20) depend strongly upon the choice of the coordinate axes x and z. Since there is no symmetry requirement for choosing these axes, we shall choose the most convenient which is the axes that makes c = 0. This is convenient because it eliminates one variable and the axes will be approximately the same as the principal axes of the A tensor since the major contribution to off-diagonal terms in the A comes from the admixture of d_{xz} into the ground state. Also this choice eliminates terms involving a_1, b_1, c_1, a_2, b_2 and c_2 from the resulting equations so that only two independent orbital coefficients (b and f) will appear in these equations.

The g values are then found by operating within the ground state doublet $\psi_\pm$ with the magnetic Zeeman operator, $\beta \vec{H} \cdot (\vec{\ell} + 2.0023\vec{s})$ and this gives:

$$g_z = 2.0023 - 8b^2[\eta_2 + f^2(\eta_1 - \eta_2)]$$

$$g_x = 2.0023 - 2(\sqrt{3}a + b)^2[\eta_1 + f^2(\eta_2 - \eta_1)]$$

$$g_y = 2.0023 - 2(\sqrt{3}a - b)^2\eta_3 \tag{21}$$

$$g_{xz} = 4bef(\sqrt{3}a + b)(\eta_2 - \eta_1)$$

where g_{xz} is the off-diagonal element of g tensor in the xz plane and $\eta_1 = \xi/\Delta E_{yz}$; $\eta_2 = \xi/\Delta E_{xy}$; $\eta_3 = \xi/\Delta E_{xz}$.
Similarly the A values were found by McGarvey[42] to be:

$$A_z = -K + P\{(4/7)(1 - 2b^2) + (\eta_3/7)(\sqrt{3}a - b)(\sqrt{3}a+3b)$$
$$+ (1/7)(\sqrt{3}a + b)(\sqrt{3}a - 3b)[\eta_1 + f^2(\eta_2 - \eta_1)]$$

$$+ (g_z - 2.0023)\};$$

$$A_x = -K + P\{-(2/7)(1 - 2b^2) - (4\sqrt{3}/7)ab - (4\sqrt{3}/7)ab$$
$$\times [\eta_2 + f^2(\eta_1 - \eta_2)] - (\eta_3/7)(\sqrt{3}a - b)(\sqrt{3}a+3b)$$
$$+(g_x - 2.0023)\};\qquad\qquad\qquad (22)$$

$$A_y = -K + P\{-(2/7)(1 - 2b^2) + (4\sqrt{3}/7)ab + (4\sqrt{3}/7)ab$$
$$\times [\eta_2 + f^2(\eta_1 - \eta_2)] - (1/7)(\sqrt{3}a + b)(\sqrt{3}a-3b)$$
$$\times [\eta_1 + f^2(\eta_2 - \eta_1)] + (g_y - 2.0023) ;$$

$$A_{xz} = (2/7)efbP(\eta_2 - \eta_1)(15\sqrt{3}a + 11b);$$

$$A_{zx} = 2efP(\eta_2 - \eta_1)[2b(a + \sqrt{3}b) - (a/7)(3a + \sqrt{3}b)]$$

where $P = 2.0023g_N\beta_e\beta_N < r^{-3}>_{ave}$ and K is the Fermi contact term. In deriving equations (21) and (22) it was assumed that $\xi/\Delta E_{x^2-y^2} \approx \eta_3$. This quantity may be approximated because it appears only in terms whose values are small.

To diagonalize the g tensor, the x and z axes must be rotated. The angle through which they must be rotated is given by:

$$\tan 2\phi = 2g_{xz}/(g_x - g_z) \qquad\qquad (23)$$

To solve for seven unknowns in equations (21) and (22), it was assumed that the values of A_x, A_y, A_z, g_x, g_y and g_z are the same as the principal values determined experimentally and that ϕ is equal to the angle between the principal z axes for the g and A tensors. Equations (21) and (22) were solved by successive approximations. A_z was assumed positive and A_x and A_y negative since assumine A_z negative resulted in a smaller

value for P indicating considerable delocalization of the unpaired electron. The values of the parameters obtained by the solution of the above equations are given in Table 10. In obtaining the parameters given in this Table, it was assumed that the difference between the coordinate systems of equations (21) and (22) and the principal axes of the $\underset{\sim}{A}$ tensor was negligible. This assumption can be checked by using these parameters to calculate the angle $\phi(A)$ between the principal z axis and the coordinate z axis. The angle of rotation needed to diagonalize the hyperfine term of equation (22) is given by:

$$\tan 2\phi(A) = \frac{2(A_z A_{zx} + A_x A_{xz})}{A_z^2 - A_x^2 + A_{xz}^2 - A_{zx}^2} \qquad (24)$$

Using the parameters given in Table 10 a value of 0.14° is obtained for $\phi(A)$, which is less than the experimental error.

The above analysis is similar to that done by Kosky et al.[4] for MnO_4^{2-} in $BaSO_4$ and by Banks et al.[5] for CrO_4^{3-} in Ca_2PO_4Cl except for the assumption of a lower symmetry. These workers did not detect any difference in the principal axes of the $\underset{\sim}{g}$ and $\underset{\sim}{A}$ values and therefore assumed an effective symmetry of C_{2v} which requires $f = 0$ in equations (21) and (22). The results of their analysis are also given in Table 10 for comparison with the results obtained in this study. In these analyses the unpaired electron was found to be located primarily in a d_z2 orbital. The values of b^2 found for MnO_4^{2-} in both $BaSO_4$ and $BaSeO_4$ are found to be larger than that found for CrO_4^{3-} in Ca_2PO_4Cl. These values indicate a relatively small admixture of $d_{x^2-y^2}$ orbital for CrO_4^{3-} but larger for MnO_4^{2-} in the ground state. In CrO_4^{3-} in Ca_2PO_4Cl the

TABLE 10

Electronic Parameters for MnO_4^{2-} and CrO_4^{3-}

	MnO_4^{2-}		CrO_4^{3-}	
	$BaSeO_4$ [a]	$BaSO_4$ [b]	Ca_2PO_4Cl [c]	$Ca_5(PO_4)_3Cl$ [d]
K (10^{-4} cm^{-1})	59.7	48	−31.6	−
P (10^{-4} cm^{-1})	141.7	179	−10.2	−
η_1	0.00657	0.0061	0.0081	0.011 [e]
η_2	0.127	0.12	0.21	0.32
η_3	0.00775	0.0069	0.0096	0.011 [e]
b^2	0.017	0.023	0.0053	0.009
f^2	0.0003	< 0.0001	< 0.0001	−

a. This work

b. Reference 4

c. Reference 5

d. Reference 6

e. Assumed equal in analysis

accidental equality of the terms $(\sqrt{3}a + b)^2\eta_1$ and $(\sqrt{3}a-b)^2\eta_3$ gave rise to axial symmetry. This is not so for MnO_4^{2-} in both $BaSO_4$ and $BaSeO_4$. Thus as a result of the smaller b^2 value there is a lesser admixture of $d_{x^2-y^2}$ orbital in the ground state of CrO_4^{3-} than in that of MnO_4^{2-}. For the two host lattices, $BaSO_4$ and $BaSeO_4$, the A values are highly anisotropic and this arises from the larger b^2 values. The large value of η_2 for both ions relative to the values of η_1 and η_3 confirm the assumption that ΔE_{xy} is small and hence the distortion from tetrahedral symmetry is not large.

The difference in the ground states for MnO_4^{2-} in $BaSO_4$, $BaSeO_4$ and in K_2CrO_4 is puzzling. The three host lattices belong to the same space group and their oxyanion tetrahedra have similar bond angles. Before this work was done it was thought that the different ground states of MnO_4^{2-} in $BaSO_4$ and in K_2CrO_4 could be due to shorter bond distances of SO_4^{2-}. K_2MnO_4 and $KMnO_4$ crystalise in the same space group, Pmna, and their bond angles and bond distances are listed in Table 11. The bond angles of these oxyanions are essentailly tetrahedral. The Mn-O bond distance for MnO_4^{2-} is slightly larger than those of MnO_4^-. The longer bond distance of MnO_4^{2-} is probably due to the extra electron which expands the metal ion, but does not distort the bond angles of the oxyanion. In K_2CrO_4, $BaSO_4$ and $BaSeO_4$ the bond angles are similarly distorted from the tetrahedral angles. The bond distances of SeO_4^{2-}[41] and CrO_4^{2-} are slightly shorter than those of MnO_4^{2-} while that of SO_4^{2-} is much shorter. Thus in the substitution of MnO_4^{2-} in $BaSO_4$ the distortion could have resulted in a different anisotropy and

TABLE 11

Bond Angles and Bond Distances for MnO_4^{2-} and MnO_4^{-} Tetrahedra

Bond Angles	Bond Distances

MnO_4^{2-} (a)

$O_{III} - Mn - O_{III}$	$109°$	$Mn - O_{III}$ 1.66 Å
$O_{III} - Mn - O_{I}$	$110°$	$Mn - O_{I}$ 1.65 Å
$O_{I} - Mn - O_{II}$	$110°$	$Mn - O_{II}$ 1.67 Å
$O_{II} - Mn - O_{III}$	$108°$	

MnO_4^{-} (b)

$O_{III} - Mn - O_{III}$	$109°$	$Mn - O_{III}$ 1.63 Å
$O_{III} - Mn - O_{I}$	$109°$	$Mn - O_{I}$ 1.62 Å
$O_{I} - Mn - O_{II}$	$111°$	$Mn - O_{II}$ 1.63 Å
$O_{II} - Mn - O_{III}$	$109°$	

(a) G. Palenik, Inorg. Chem. 6 , 503 (1967)

(b) M. Greenblatt, E. Banks, and B. Post, Acta Crystallogr.

23, 166 (1967)

hence a different ground state. Both SeO_4^{2-} and CrO_4^{2-} have
comparable lattice size yet MnO_4^{2-} has the same ground state in
$BaSeO_4$ as in $BaSO_4$. Thus the different ground state in K_2CrO_4
cannot be due solely to the difference in the size of the host
anion.

B. Molecular Orbital Theory:

In the previous studies of MnO_4^{2-} in $BaSO_4$ and K_2CrO_4
the authors did not perform a molecular orbital analysis to
determine the charge transfer in the Mn-O bond. Because of the
accuracy in the determination of the spin Hamiltonian parameters
in this study, a molecular orbital analysis similar to that
done by McGarvey[30] on CrO_4^{3-} was carried out to determine the
charge transfer in the MnO_4^{2-}. The coordinate axes in the complex
are taken to be those shown in Figure 13. The angle θ is chosen
so that the z axis is an improper rotation axis for the D_{2d}
symmetry while the x and y axes are in the mirror plane. In
MnO_4^{2-}, the Mn(VI) is surrounded by four oxygen atoms in a
distorted tetrahedral configuration. Each oxygen atom is assumed
to have available the $2p_x$, $2p_y$ and $2p_z$ orbitals for the formation
of molecular orbitals with the d orbitals of the central ion.
The molecular orbitals are chosen for the D_{2d} symmetry since
it is assumed that these are good enough for our calculations.
the localized antibonding molecular orbitals are :

$$A_1 = \beta_{z^2}d_{z^2} - (1/2)\beta'_{z^2}(p_x^1 - p_x^2 - p_x^3 + p_x^4);$$

$$E_{xz} = \alpha_{xz}d_{xz} + (\alpha'_{xz}/2)\cos\omega(p_z^1 - p_z^4) - (\alpha'_{xz}/2\sqrt{2})\sin\omega$$

$$\times(p_x^1 - p_x^4 - \sqrt{3}p_y^2 + \sqrt{3}p_y^3);$$
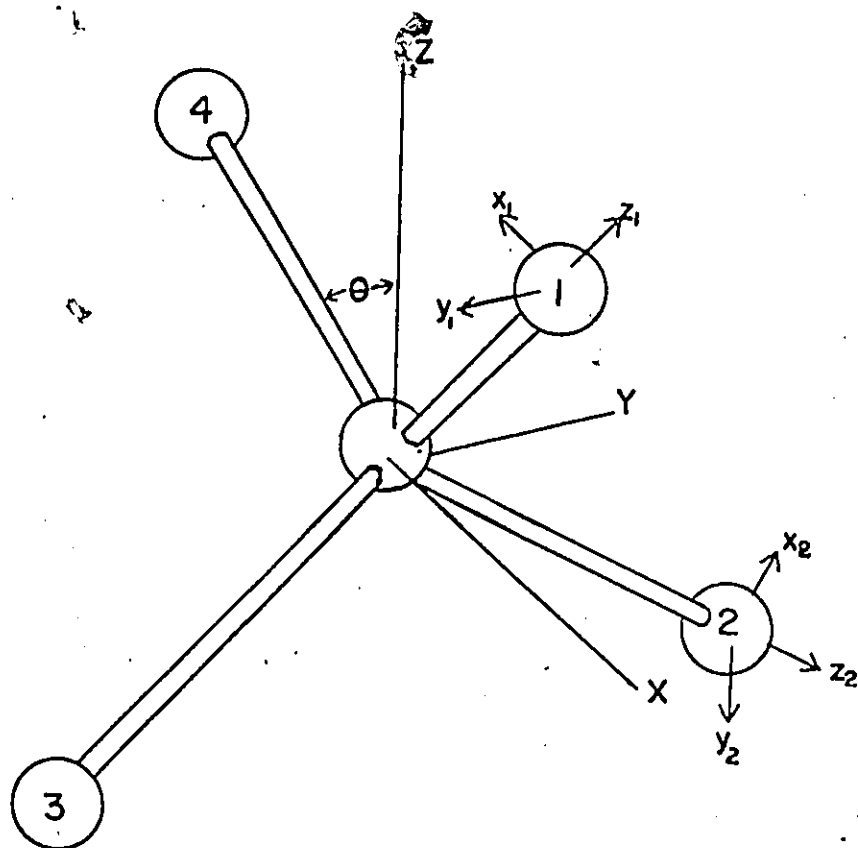
Figure 13. Coordinate axes used in the MO calculations for MnO_4^{2-}

$$E_{yz} = \alpha_{yz}d_{yz} - (\alpha'_{yz}/\sqrt{2})\cos\omega(p_z^2 - p_z^3) - (\alpha'_{yz}/2\sqrt{2})\sin\omega$$
$$\times(p_x^3 - p_x^4 - \sqrt{3}p_y^1 + \sqrt{3}p_y^4); \qquad (25)$$

$$B_1 = \alpha_{x^2-y^2}d_{x^2-y^2} - (\alpha'_{x^2-y^2}/2)\cos\rho(-p_x^1-p_x^2-p_x^3-p_x^4)$$
$$- (\alpha'_{x^2-y^2}/2)\sin\rho(-p_z^1 + p_z^2 + p_z^3 - p_z^4);$$

$$B_2 = \beta_{xy}d_{xy} - (\beta'_{xy}/2)(-p_y^1 + p_y^2 + p_y^3 - p_y^4)$$

The angles ω and ρ are molecular orbital parameters and their values are chosen to maximize the overlap integrals. The orbitals are designated by the irreducible representations of the D_{2d} symmetry to which they belong. In the previous work on CrO_4^{3-} it was assumed that distortion from tetrahedral symmetry was so small that α_{xz} is equal to both α_{yz} and $\alpha_{x^2-y^2}$ and that β_{z^2} is equal to β_{xy}. The analysis was then done in terms of the simpler equations applicable to the axial symmetry of D_{2d}. In this approach $g_\perp$ and $A_\perp$ were obtained by averaging the experimental x and y values. This calculation was done for MnO_4^{2-} in $BaSO_4$ and $BaSeO_4$ and the resulting charges for the manganese ion are reported later in Tables 13 and 14 as U_{axial}. The larger anisotropies observed for MnO_4^{2-} suggested that an alternative method of calculation might be appropriate.

The parameters that were obtained in the previous analysis and listed in Table 10 may be approximately calculated from the molecular orbitals in the following manner:

$$P = 2.0023 g_N \beta_e \beta_N <A_1|r^{-3}|A_1> = \beta_{z^2}^2 P_d$$

$$P_d = 2.0023 \ g_N \beta_e \beta_N < d_{z^2}|r^{-3}|d_{z^2}> \tag{26}$$

$$\eta_1 = (1/3)<A_1|\ell_x|E_{yz}><E_{yz}|\ell_x|A_1>/\Delta E_{yz}$$

$$= (\xi_d/\Delta E_{yz})\{P_\pi(z^2)P_\sigma(yz)-\alpha_{yz}\alpha'_{yz}\beta_{z^2}\beta'_{z^2}[\cos\omega-(\sqrt{3}/2)$$

$$\times \sin\theta\sin\omega]/\sqrt{6}\} \tag{27a}$$

$$\eta_2 = (1/4)<A_1|\ell_z|B_2><B_2|\ell_z|A_1>/\Delta E_{xy}$$

$$= (\xi/\Delta E_{xy})\{P_\pi(xy)P_\sigma(x^2-y^2)-\alpha_{x^2-y^2}\alpha'_{x^2-y^2}\beta_{xy}\beta'_{xy}$$

$$\times (\sin\theta\sin\rho-\cos\theta\cos\rho)/2\} \tag{27b}$$

$$\eta_3 = (1/3)<A_1|\ell_y|E_{xz}><E_{xz}|\ell_y|A_1>/\Delta E_{xz}$$

$$= (\xi/\Delta E_{xz})\{P_\pi(z^2)P_\sigma(xz)-\alpha_{xz}\alpha'_{xz}\beta_{z^2}\beta'_{z^2}[\cos\omega-\sqrt{3}/2$$

$$\times \sin\theta\sin\omega]/\sqrt{6}\} \tag{27c}$$

where ξ_d is the spin orbit coupling constant for the d electron
and P_σ and P_π are the charge densities on the manganese ion
in the E and A_1 orbitals respectively. Mulliken[43]
defined these terms as:

$$P_\sigma = \alpha^2 - \alpha\alpha' s_A;$$

$$P_\pi = \beta^2 - \beta\beta' s_E$$

α, α', β and β' have been defined in equation (25) s_A and s_E
are the overlap integrals whose values have been calculated
from the overlap integrals of Jaffe[44] and Jaffe and Doak[45]
who gave the values of the integrals $\int d_z 2 p_x^1 d\tau$ and $\int d_{yz} p_z^2 d\tau$.
The spin orbit contribution of the ligand oxygen atom has not
been taken into account because of its relatively small value
compared to that of the manganese ion. The angle 2θ is the

angle between two bonds and is taken as 109.5° for these calculations. Following the procedure of McGarvey[30] the contribution of the excited state, arising from the promotion of a bonding electron in the $^\ddagger E_{xz,yz}$ orbital to the A_1 orbital, to the spin Hamiltonian parameters is considered. The wave function of the $^\ddagger E_{yz}$ bonding molecular orbital is given as:

$$^\ddagger E_{yz} = {}^\ddagger \alpha d_{yz} + ({}^\ddagger \alpha'/\sqrt{2})\cos\omega (p_z^2 - p_z^3) + ({}^\ddagger \alpha'/2\sqrt{2})\sin\omega$$
$$(p_x^2 - p_x^3 - \sqrt{3}p_y^1 + \sqrt{3}p_y^4) \tag{28}$$

The additional contribution to the parameter η_1 is:

$$\Delta\eta_1 = -(\xi_d/\Delta E_{yz}^\ddagger)\{P_\pi(z^2)[1 - P_\sigma(yz)] + {}^\ddagger\alpha_{yz}{}^\ddagger\alpha'_{yz}\beta_z 2\beta'_z 2$$
$$\times [\cos\omega - (\sqrt{3}/2)\sin\theta\sin\omega]/\sqrt{6}\} \tag{29}$$

Similar expressions are obtained for $\Delta\eta_2$ and $\Delta\eta_3$. In obtaining equation (29) use was made of the fact that the orthogonality of E_{yz} and $^\ddagger E_{yz}$ requires that

$$(1 - P_\sigma) = {}^\ddagger\alpha^2 - {}^\ddagger\alpha\alpha' s_E \tag{30}$$

The number of electrons in the metal d orbitals of the σ bonding orbitals is

$$6 - 2P_\sigma(xy) - 2P_\sigma(yz) - 2P_\sigma(x^2-y^2)$$

and for the bonding π orbitals is

$$4 - 2P_\pi(xy) - 2P_\pi(z^2).$$

The effective charge, Q, on the manganese ion is given by:

$$Q = -3 + 2P_\sigma(xz) + 2P_\sigma(yz) + 2P_\sigma(x^2-y^2) + 2P_\pi(xy) + 2P_\pi(z^2) \tag{31}$$

From this molecular orbital analysis the only values that can be determined are those of $P_\pi(z^2)$, $P_\sigma(xz)$ and $P_\sigma(yz)$. $P_\pi(xy)$ has, therefore, been estimated as equal to $P_\pi(z^2)$ while $P_\sigma(x^2-y^2)$ has been taken as the average of the values of

$P_\sigma(xz)$ and $P_\sigma(yz)$. The values of the spin orbit coupling constant, ζ_d, for the d orbitals of manganese ion can be calculated from the spectroscopic tables[46] and the values of P_d can be determined from Hartree-Fock computations[47]. The values of ΔE_{xz} and ΔE_{yz} for MnO_4^{2-} in $BaSO_4$ have been obtained from spectroscopic studies[4] and the same values have been assumed for MnO_4^{2-} in $BaSeO_4$ crystals. Overlap integrals can be estimated from tables[44,45] using shielding parameters obtained by Clementi and Raimondi[48]. The values of these parameters used in the computations are given in Table 12. Following the work[30] on CrO_4^{3-}, a self consistent method in which the values of the parameters given in Table 12 for an assumed charge are used to calculate the charge density in each orbital. This calculated charge density is then compared with the assumed charge. The values of Q and charge densities in the individual molecular orbitals obtained by using equation (31) are given in Table 13 for the case of $\Delta E_{xy,yz}$ equal to infinity and $\Delta E^{\ddagger}_{xz,yz}$ equal to 33,000 cm^{-1}. Values of Q obtained using the axial approximation employed on CrO_4^{3-} are given for comparison. For MnO_4^{2-} in $BaSO_4$ there is no solution of the equation for an assumed charge of +1. The values of Q obtained from the self consistent method and the molecular charge densities are given in Table 14. The values of Q and Q_{axial} are seen to be very similar indicating that their determination is not too sensitive to the different approximations used in the two methods of computation. The values of P_σ are found to be slightly higher when estimated by the axial approximation and the values of P_π are lower

TABLE 12

Parameters used in MO Computations

Charge	+1	+2	+3	+4
ξ_d (cm^{-1})	248	297	361	405
P_d (10^{-4} cm^{-1})	163	187	211	235
s_A	0.046	0.044	0.042	0.039
s_E	0.142	0.134	0.125	0.118
ΔE_{xz} (cm^{-1})		10,064		
ΔE_{yz} (cm^{-1})		9,813		
$\Delta E_{xz,yz}^{\ddagger}$ (cm^{-1})		$\geq$33,000		

TABLE 13

MO Results for MnO_4^{2-} in $BaSO_4$ and $BaSeO_4$

Assumed Charge	$\Delta E_{xz,yz}^{\ddagger}$ (cm^{-1})	$P_\sigma(xz)$	$P_\sigma(yz)$	$P_\pi(z^2)$	Q	Q_{axial}
			$BaSeO_4$			
+4	∞	0.474	0.415	0.583	1.418	1.656
+3	∞	0.457	0.398	0.651	1.515	1.689
+2	∞	0.461	0.397	0.738	1.790	1.916
+1	∞	0.445	0.379	0.852	2.028	2.114
+4	33,000	0.619	0.578	0.583	2.340	2.457
+3	33,000	0.604	0.561	0.651	2.447	2.522
+2	33,000	0.603	0.557	0.738	2.696	2.739
+1	33,000	0.587	0.538	0.852	2.930	2.949
			$BaSO_4$			
+4	∞	0.325	0.291	0.744	1.081	1.135
+3	∞	0.304	0.270	0.832	1.215	1.229
+2	∞	0.288	0.252	0.946	1.458	1.481
+4	33,000	0.505	0.481	0.744	2.188	2.170
+3	33,000	0.484	0.459	0.832	2.324	2.283
+2	33,000	0.464	0.437	0.946	2.543	2.575

TABLE 14

Self Consistent Values for MnO_4^{2-}

$\Delta E^{\ddagger}_{xz,yz}$	Q	Q_{axial}	$P_\sigma(xz)$	$P_\sigma(yz)$	$P_\pi(z^2)$
		$BaSeO_4$			
∞	1.830	1.930	0.458	0.394	0.757
33,000	2.557	2.607	0.604	0.559	0.690
		$BaSO_4$			
∞	1.564	1.585	0.281	0.244	0.996
33,000	2.445	2.445	0.473	0.447	0.895

but the differences are not large. The value of $\Delta E^{\ddagger}_{xz,yz}$ is
not known but the value of 33,000 cm^{-1} assumed is not
unreasonable on the basis of the spectroscopic studies[4]
and the values of ν obtained with it are therefore, thought
to be close to the correct values.

Tables 13 and 14 show that the effective charge on
Mn(VI) ion is about 2. Since the effective charge is lowered
the d orbital radius increases as the covalency of the bond
increases. The P value defined in equation (26) is proportional
to r^{-3}. Hence the P value will decrease with increasing
charge transfer. The P values are 287x10^{-4} cm^{-1} for Mn(VI)
ion and 189x10^{-4} cm^{-1} for Mn(II) ion. The experimental values
of 141.7x10^{-4} cm^{-1} for MnO_4^{2-} in $BaSeO_4$ and 179x10^{-4} cm^{-1} for
MnO_4^{2-} in $BaSO_4$ indicate that the effective charges are more
nearly +2 than the formal charge of +6. It appears that for
MnO_4^{2-} the high oxidation number requires some charge transfer
to stabilize the complex ion. Although the effective charge
on manganese is the same in both $BaSeO_4$ and $BaSO_4$ lattices,
there is a change in the pattern in which the charge transfer
takes place. Table 10 shows that more charge transfer takes
place through the σ orbitals and less through the π orbitals
when MnO_4^{2-} substitutes for the smaller SO_4^{2-} ion than when
it substitutes for the larger SeO_4^{2-} ion. Very little charge
transfer via the π orbitals is indicated in the $BaSO_4$ by the
data.

C. The Molecular Orbital Approach to the Analysis of the Spin

Hamiltonian Parameters for $Fe(CN)_5NH_3^{2-}$ in $Na_2Fe(CN)_5NO.2H_2O$:

In the previous studies on strong field t_{2g}^5 systems[9-16] it was always assumed that distortions from octahedral symmetry were of the type that kept the principal axes coincident with the bond axes and, therefore, the appropriate d orbitals to be used in the theory were d_{xy}, d_{xz} and d_{yz}. The system studied here does not meet this condition since the site symmetry requires that the x and y axes bisect the equatorial Fe - CN bond angles. There is only one plane of symmetry in the host crystal, but C_{2v} symmetry will be assumed in the following discussion. The molecular orbitals for the t_{2g} set of orbitals can be written as:

$$|x^2-y^2> = \alpha d_{x^2-y^2} - (\alpha_1/2)(p_x^3 + p_x^4 - p_x^5 - p_x^6)$$

$$- (\alpha_2/2)(-p_y^3 + p_y^4 - p_y^5 - p_y^6)$$

$$|xz> = \beta d_{xz} - (\beta_1/2)(p_z^3 + p_z^4 - p_z^5 - p_z^6)$$

$$- \beta_2 p_x^1 + \beta_3 p_x^2$$

$$|yz> = \gamma d_{yz} - (\gamma_1/2)(p_z^3 - p_z^4 + p_z^5 - p_z^6)$$

$$- \gamma_2 p_y^1 + \gamma_3 p_y^2$$

(32)

The coordinate axes are those shown in Figure 14. The z axis is along the $Fe-NH_3$ bond axis while the x and y axes are in the molecular plane. If now the spin orbit coupling and tetragonal distortion effects are taken into account the two
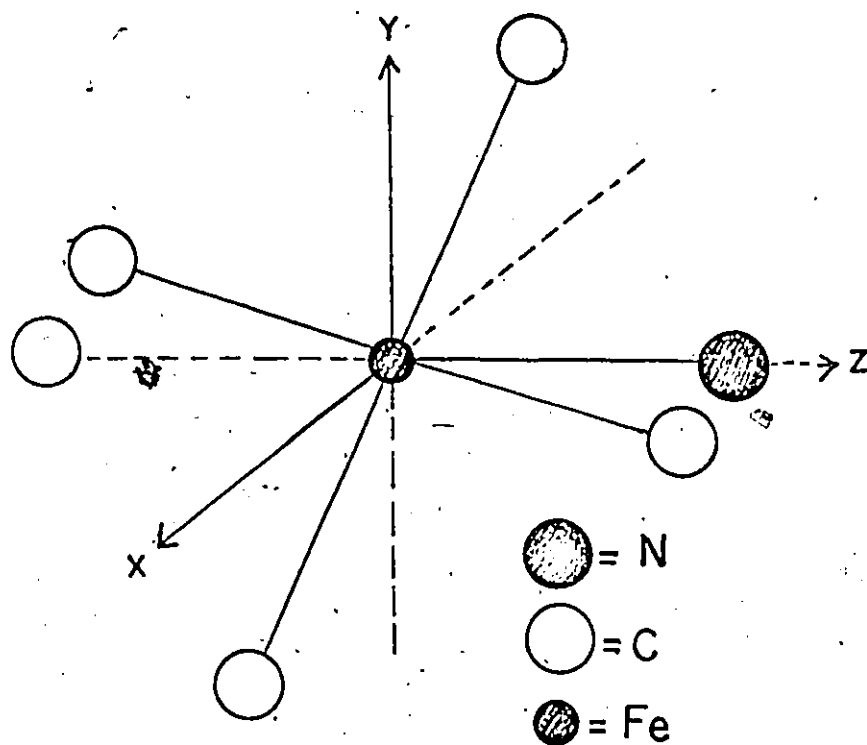
Figure 14. Coordinate axes used in the MO calculations for $Fe(CN)_5NH_3^{2-}$.

Kramers doublets can be written as :

$$\psi_+ = d|xz+> + ie|yz+> - f|(x^2-y^2)->$$

$$\psi_- = d|xz-> - ie|yz-> - f|(x^2-y^2)+> \tag{33}$$

where $|xz+>$ represents the molecular orbital with $+1/2$ spin belonging to the irreducible representation of ψ_{xz}. The one electron hole formalism is used here to represent the t_{2g}^5 configuration. The constants d, e and f are found by degenerate perturbation theory to be

$$f = \frac{\eta_2}{\eta_3} \frac{-\left[\frac{1}{2}\frac{\eta_1\eta_3}{\eta_2} - E\right]}{\left[1 + \frac{1}{2}\varepsilon + \frac{1}{2}\frac{\eta_1\eta_2}{\eta_3} - E\right]} d \tag{34a}$$

$$e = \frac{2}{\eta_3} \frac{\{(1/4)\eta_1^2 + [1 + (1/2)\varepsilon]E - E^2\}d}{\left[1 + (1/2)\varepsilon + (1/2)(\eta_1\eta_2/\eta_3) - E\right]} \tag{34b}$$

$$d^2 + e^2 + f^2 = 1 \tag{34c}$$

$$E = (1/3)[1 + (3/2)\varepsilon)] + X \tag{34d}$$

where

$$X = (2/3)[1+(3/4)\varepsilon^2+(3/4)(\eta_1^2+\eta_2^2+\eta_3^2)] \cos(\phi/3,\phi/3+120,\phi/3+240)$$

$$\cos\phi = [1-(9/4)\varepsilon^2+(9/8)(\eta_1^2-\eta_3^2)+(9/8)(\eta_2^2-\eta_3^2)-(27/16)\varepsilon(\eta_1^2-\eta_2^2)$$

$$-(27/8)\eta_1\eta_2\eta_3]/[1+(3/4)\varepsilon^2+(3/4)(\eta_1^2+\eta_2^2+\eta_3^2)]^{(3/2)}$$

$$\eta_1 = \xi_1/\Delta; \quad \eta_2 = \xi_2/\Delta; \quad \eta_3 = \xi_3/\Delta \text{ and } \varepsilon = \delta/\Delta$$

$$\Delta = E_{x^2-y^2} - (E_{xz} - E_{yz})/2 \text{ and } \delta = E_{yz} - E_{xz}$$

The spin orbit coupling constants ξ_n are defined as

$$\xi_1 = \alpha\gamma\xi_{3d}; \quad \xi_2 = \alpha\beta\xi_{3d}; \quad \xi_3 = \beta\gamma\xi_{3d}.$$

$E_{x^2-y^2}$ is the energy of the $|x^2-y^2>$ orbital while E_{yz} and

E_{xz} are the energies of $|yz>$ and $|xz>$ molecular orbitals in the absence of the spin orbit coupling.

Since only three g values are obtained experimentally, it has been necessary in the following analysis of the g values to make the usual simplifying assumption that

$$\eta_1 = \eta_2 = \eta_3.$$

From equation (33) the following expressions for the g values can be obtained

$$g_x = 2.0023(d^2 - e^2 - f^2) - 4efk$$
$$g_y = 2.0023(d^2 - e^2 - f^2) + 4efk \qquad (35)$$
$$g_z = 2.0023(d^2 + e^2 - f^2) + 4dek$$

where $k = i<xz|\ell_z|yz> = i<yz|\ell_x|x^2-y^2> = i<xz|\ell_y|x^2-y^2>$. Consistent with the assumption about η, it has been assumed that k, the orbital reduction parameter, is the same for all three molecular orbitals. In deriving equation (35), it was also assumed that the second order contribution from the e_g orbitals can be neglected compared to the very large first order contributions from the t_{2g} orbitals.

Using the experimental values of g, equation (35) can be solved for d, e, f and k. Furthermore from d, e, and f, values can be obtained for η and ϵ using equation (34). The magnitude of g_z can be as large as 3.0 only if f in equation (35) is small and this is so if η is positive. ϵ must also be positive to keep $|g_y|$ greater than $|g_x|$. Only two solutions are possible for equations (34) and (35), one for g_x assumed positive and the other for it assumed negative. Assuming g_x negative gives a k value greater than unity and therefore this solution is rejected. The values obtained for the para-

meters are given in Table 15.

The value of k obtained in this study is close to 0.875, the value reported by Bleaney and O'Brien for $Fe(CN)_6^{3-}$ [10]. Oosterhuis[50] has studied the Moessbauer hyperfine spectrum of powdered $Na_2Fe(CN)_5NH_3 \cdot H_2O$ and fitted his results to equations similar to those developed here. Although he assumed the $|xy>$ orbital to be the lowest in energy, his results would equally well fit the above interpretation with the parameters: d=0.90, e=0.42, f=0.15 which are surprisingly close to the values obtained in the present study.

The values of Δ and δ could not be obtained without an independent determination of the spin orbit coupling parameter ξ. Haberditzl et al.[51] have reported the magnetic moment of iron in $Na_2Fe(CN)_5NH_3 \cdot H_2O$ to be 2.32 Bohr magnetons at $295^\circ K$. Our values of k, η and ϵ will predict this value when the value of the spin orbit coupling parameter is 325 cm^{-1} which is fairly close to 278 cm^{-1} reported by Bleaney and O'Brien[10] for $Fe(CN)_6^{3-}$. Since the free ion values of the spin orbit parameter for Fe^{2+} and Fe^{3+} are 400 and 460 cm^{-1} respectively[52], the value obtained in this study indicates considerably more covalency than the value of k would indicate.

Thornley[53] and Cotton[54] have shown that the neglect of configuration interaction in the theoretical treatment of octahedral complexes produces k values that seriously underestimate the covalency. The values of Δ, σ and the energy of the excited Kramers doublet are found to be:

TABLE 15

Molecular Orbital Parameters for $Fe(CN)_5NH_3^{2-}$

$$k = 0.893$$

$$d = 0.891$$

$$e = 0.385$$

$$f = 0.241$$

$$\eta = 0.578$$

$$\varepsilon = 0.656$$

$$\Delta = 560 \text{ cm}^{-1}$$

$$\delta = 500 \text{ cm}^{-1}$$

$$E_2 - E_1 = 530 \text{ cm}^{-1}$$

$$E_3 - E_1 = 930 \text{ cm}^{-1}$$

if $\zeta = 325 \text{ cm}^{-1}$. E_1 is the energy of the lowest Kramers doublet.

The most surprising aspect of the above results is the ground state. It is generally acknowledged that the ligand field strength of NH_3 is considerably less than that of CN^-, so that one would have expected the $|x^2-y^2\rangle$ hole orbital to be the most stable instead of the least stable as found here. Also the fact that δ is comparable to Δ is unexpected since the structure of the host lattice, $Fe(CN)_5NO^{2-}$, approximates four fold symmetry so well. The stability of the $|xz\rangle$ and $|yz\rangle$ holes over the $|x^2-y^2\rangle$ hole could be explained in part by noting that the bond angle between Fe-N-O and the equatorial Fe-C-N bonds is 96° and assuming that the $Fe(CN)_5NH_3^{2-}$ ion adopts this geometry when incorporated in the same lattice. Such a distortion stabilizes the $|xz\rangle$ and $|yz\rangle$ orbitals and destabilizes the $|x^2-y^2\rangle$ orbital. It is hard to accept this as a valid explanation because it is difficult to believe that such a small distortion is more important energetically than the difference in ligand field strengths between NH_3 and CN^-. Further if such distortions are so important, it is hard to understand why the Moessbauer results[50] for $Na_2Fe(CN)_5NH_3 \cdot H_2O$ agree so well with the results obtained in this study since the ion is in different lattices. Thus it is diffcult to avoid the conclusion that

the NH_3 group in this complex is acting as a more basic ligand than it appears to do in other complexes.

D. The Nitrogen Hyperfine Interaction:

Using the two Kramers doublets given in equation (33) and the appropriate hyperfine operators the spin Hamiltonian parameters for the hyperfine interaction were obtained by McGarvey[42] as:

$$A_x = (d^2-e^2)K_{xz}-f^2K_{x^2-y^2}+(2d^2+e^2-3ed)P_L$$
$$-(d^2-e^2-f^2-2ef)P_M$$

$$A_y = (d^2-e^2)K_{xz}-f^2K_{x^2-y^2}-(d^2+2e^2-3ed)P_L$$
$$-(d^2-e^2+f^2-2ed)P_M \qquad (36)$$

$$A_z = (d^2+e^2)K_{xz}-f^2K_{x^2-y^2}-(d^2+e^2-10ed)P_L$$
$$+ 2(d^2+e^2-f^2+2ed)P_M$$

where $P_L = (2/5)g_eg_N\beta_e\beta_N < r^{-3} >_{2p}\beta_L^2$ and

$$P_M = g_eg_N\beta_e\beta_NR^{-3}\beta^2$$

g_e and g_N are the electronic and nuclear g factors, β_e and β_N are the Bohr and nuclear magnetons respectively, $<r^{-3}>_{2p}$ is the average value of r^{-3} in a nitrogen 2p orbital and R is the Fe-N internuclear distance. K_{xz} is the Fermi contact interaction induced by the spin in $|xz>$ or $|yz>$ orbitals and $K_{x^2-y^2}$ is the interaction induced by the spin in the $|x^2-y^2>$ orbital. In equation (32) the assumption is made that β is equal to both α and γ while β_L is equal to β_2 and γ_2 of the ligand molecular orbitals.

The analysis of the hyperfine interaction is difficult because reliable values of A_x and A_y are not available neither are the signs for any of the hyperfine terms. Reasonable estimates of K_{xz} and P_L could be arrived at by considering the range of possible solutions for equation (36). P'_M is small and can be readily estimated to be 0.26×10^{-4} cm^{-1} by assuming $R = 1.95$ Å and β^2 equal to unity. It is readily established that positive values of P_L are only possible if A_z is positive. Further studies[20,55] of the hyperfine interaction of ^{13}C and ^{14}N in $Cr(CN)_5NO^{3-}$ show that K_{xz} and $K_{x^2-y^2}$ are negative and that $|K_{x^2-y^2}|$ is less than $|K_{xz}|$. If this restriction is placed on the above solutions, it is found that A_x must be positive and A_y negative and P_L must be between 2.7×10^{-4} cm^{-1} and 5.0×10^{-4} cm^{-1} to be consistent with the above results. K_{xz} must be between 0 and -5.0×10^{-4} cm^{-1} with the larger magnitude values associated with the smaller values of P_L

Morton[56] has reported a value of 3.101 a. u. for $\langle r^{-3} \rangle_{2p}$ which would make P_L equal to 15.9×10^{-4} cm^{-1} if β_L^2 is equal to one. Thus the experimental estimates of P_L predict values of β_L^2 between 0.17 and 0.31. This is a larger covalency than normally found in metal-ammonia bonds, but is however consistent with the conclusion in this study from g values that the NH_3 is interacting more strongly than one would expect.

This conclusion seems difficult to accept and appears more plausible if the NH_3 has lost a proton to become NH_2^- which is a much stronger base than NH_3. Herington[57,58]

has reported the reaction of pentacyanoammino ferrate(III)
with aromatic amines and claimed the formation of complicated
complexes. Thus with aniline, $Na_2Fe(CN)_5NH_3.H_2O$ forms
$Na_3Fe(CN)_5.NH.C_6H_4NHPh$. The possibility of the formation of
$Na_2Fe(CN)_5NH_2.H_3^+O$ was made probable by the fact that
$Na_2Fe(CN)_5NH_3.H_2O$ undergoes color changes from reddish-yellow
in strongly alkaline solutions to deep blue in acidic solutions.
Attempts to determine this acid-base equilibrium by measuring
the NMR shift of the amine hydrogen as a function of pH
failed because water was in such a high concentration that
the rapid exchange between the amine hydrogen and the water
protons made it impossible to observe any resonance due to
the amine hydrogen. In order to determine whether NH_3 was
present in the solid $Na_2Fe(CN)_5NH_3.H_2O$ as NH_2^- with the
proton abstracted by the water of hydration, a broad line NMR
study of the powder was undertaken. The spectrum recorded
at room temperature is shown in Figure 15. This spectrum
shows a pattern typical of two protons and a sharp resonance
at the center. The two proton pattern was analyzed and fitted
to that expected for two protons separated by a distance of
1.62 Å, a value equivalent to that found in hydrates. The
central resonance line has a wing typical of an axially
symmetrical system that has a perpendicular and parallel shifts.
Since water of hydration is normally hydrogen bonded and
does not move freely, it is unlikely that the sharp resonance
can be attributed to the hydronium ion. Thus it appears that
the sharp resonance must be due to the NH_3 which is not

Figure 15. Broad line NMR spectrum of powdered Na$_2$Fe(CN)$_5$NH$_3$.H$_2$O at rocm temperature

expected to be rigidly bound. It is, therefore, inevitable to conclude that the ammino group is not present as NH_2^- in this complex.

That the NH_3 is interacting strongly in this complex could be understandable by considering the role of the CN^- ion. The cyanide ion has a pair of degenerate, normally unoccupied, antibonding π-orbitals. These have the appropriate symmetry to combine with t_{2g} orbitals of the iron. These π-orbitals enable the cyanide ion to act as an electron acceptor. This increases the effective charge on the iron and hence results in a stronger interaction between the NH_3 and the iron.

Chapter VIII

CONCLUSIONS

The electron spin resonance spectra have been investigated for manganate ions in barium selenate and for amminopentacyanoferrate (III) in sodium nitroprusside. Both the crystal field theory and the molecular orbital approaches have been used to analyze the spin Hamiltonian parameters. For the manganate ions in barium selenate the spin Hamiltonian parameters are shown to be consistent only with a ground state in which the unpaired electron is in a d_{z^2} orbital with a 2% admixture of $d_{x^2-y^2}$ orbital. The difference in the principal x and z axes for the g and the A tensors has been shown to be attributed to the admixture of the d_{yz} orbital with the d_{xy} orbital. This has been estimated to be 0.03% from the angular separation of the axes. The molecular orbital coefficients, α and β, together with an estimate of the overlap integrals have been used to determine the charge densities on the metal ion. From the charge densities the formal charge on manganese was calculated by a self consistent method. It was found that the formal charge on Mn(VI) is about +2 which is in line with similar values found for other ions of high oxidation numbers [28,59,60],

One significant difference between the manganate ion in barium selenate and in barium sulfate is in the value of K, the isotropic term. This value can be used to calculate

80

χ, a quantity defined by Abragam et al.[61] as characteristic of the central density of unpaired spin as:

$$\chi = (4\pi/S) < \Psi| \sum_i \delta(r_i) S_{zi} |\Psi >$$

χ values obtained are

$$\chi = -1.64 \text{ for } MnO_4^{2-} \text{ in } BaSO_4$$

$$\chi = -2.04 \text{ for } MnO_4^{2-} \text{ in } BaSeO_4.$$

McGarvey[49] has demonstrated that the value of χ is nearly constant for a given configuration with similar ligands unless there is mixing of 3d and 4s orbitals. Such a mixing is symmetry-forbidden for the d_{xy} ground state observed for MnO_4^{2-} in K_2CrO_4 so that the value of $\chi = -1.91$ in this system can be used as a measure of that portion of χ resulting from indirect polarization of inner s orbitals of manganese. Such a mixing would produce a positive contribution to χ. It would appear that such a mixing is negligible for MnO_4^{2-} in $BaSeO_4$ but a small admixture of about 0.1% occurs for MnO_4^{2-} in $BaSO_4$.

For $Fe(CN)_5NH_3^{2-}$ in $Na_2Fe(CN)_5NO.2H_2O$, the spin Hamiltonian parameters are shown to be consistent only with a ground state in which the unpaired electron is primarily in a d_{xz} orbital rather than the expected $d_{x^2-y^2}$ orbital. The molecular orbital analysis of the spin Hamiltonian parameters has shown that there is a larger covalency than normally found in the metal-ammonia bonds and this is consistent with the conclusion that the NH_3 is interacting more strongly in this complex than one would expect.

DERIVATION OF SECOND ORDER TERMS FOR S=1/2 IN RHOMBIC SYMMETRY

The spin Hamiltonian for this system is

$$\hat{H} = \beta(g_x H_x S_x + g_y H_y S_y + g_z H_z S_z) + A_x S_x I_x + A_y S_y I_y + A_z S_z I_z$$

We will quantize S and I in a coordinate system such that $\underset{\sim}{S} \cdot \underset{\approx}{g} \cdot \underset{\sim}{H}$
and $\underset{\sim}{S} \cdot \underset{\approx}{A} \cdot \underset{\sim}{I}$ give no off diagonal terms that involve two states
with the same eigenvalue of S.

We will choose this x'y'z' coordinate system with
different choices of $\underset{\sim}{S}$ and $\underset{\sim}{I}$.
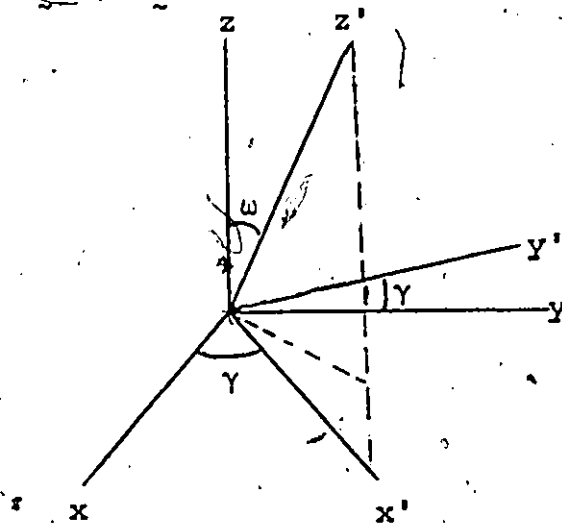
$$S_x = S_{x'}\cos\omega\cos\gamma - S_{y'}\sin\gamma + S_{z'}\sin\omega\cos\gamma$$

$$S_y = S_{x'}\cos\omega\sin\gamma + S_{y'}\cos\gamma + S_{z'}\sin\omega\sin\gamma$$

$$S_z = S_{x'}\sin\omega + S_{z'}\cos\omega$$

Now $H_x = H\sin\alpha\cos\phi$

$H_y = H\sin\alpha\sin\phi$

$H_z = H\cos\alpha$

82

so that

$$\underset{\sim}{S} \cdot \underset{\approx}{g} \cdot \underset{\sim}{H} = (g_x \sin\omega\cos\gamma\sin\alpha\cos\phi + g_y\sin\omega\sin\gamma\sin\alpha\sin\phi + g_z\cos\omega\cos\alpha)S_z$$

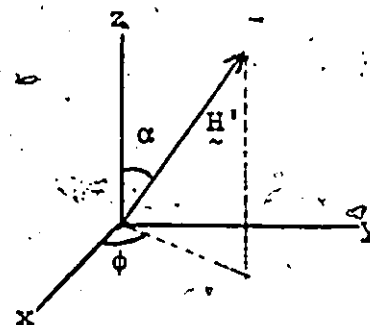$$+ (g_x\cos\omega\cos\gamma\sin\alpha\cos\phi + g_y\cos\omega\sin\gamma\sin\alpha\sin\phi - g_z\sin\omega\cos\alpha)S_x$$

$$+ (-g_x\sin\gamma\sin\alpha\cos\phi + g_y\cos\gamma\sin\alpha\sin\phi)S_y$$

The $S_{y'}$ term shall be equal to zero when

$$- g_x\sin\gamma\cos\phi + g_y\cos\gamma\sin\phi = 0$$

or when $\quad \tan\gamma = (g_y/g_x)\tan\phi$

i.e., $\quad \sin\gamma = g_x\sin\phi/(g_x^2\cos^2\phi + g_y^2\sin^2\phi)^{1/2}$

and $\quad \cos\gamma = g_x\cos\phi/(g_x^2\cos^2\phi + g_y^2\sin^2\phi)^{1/2}$

Thus $S_{x'}$ term becomes

$$(g_x^2\cos^2\phi + g_y^2\sin^2\phi)^{1/2}\cos\omega\sin\alpha - g_z\sin\omega\cos\alpha$$

which becomes zero when

$$\tan\omega = [(g_x^2\cos^2\phi + g_y^2\sin^2\phi)^{1/2}/g_z]\tan\alpha$$

Also the $S_{z'}$ term becomes

$$[g_x^2\sin^2\alpha\cos^2\phi + g_y^2\sin^2\alpha\sin^2\phi + g_z^2\cos^2\alpha]^{1/2} = g$$

Therefore $\beta\underset{\sim}{S} \cdot \underset{\approx}{g} \cdot \underset{\sim}{H}$ becomes $g\beta HS_{z'}$ and the first order solution is

$$E = \pm(1/2)g\beta H.$$

Now to keep $\underset{\sim}{S} \cdot \underset{\approx}{A} \cdot \underset{\sim}{I}$ from mixing up terms with the same eigenvalues

of $S_{z'}$ we must choose ω_I and γ_I to make the $S_{z'}I_{x'}$ and $S_{z'}I_{y'}$

terms zero. The $S_{z'}I_{x'}$ term is

$$A_x\sin\omega\cos\gamma\cos\omega_I\cos\gamma_I + A_y\sin\omega\sin\gamma\cos\omega_I\sin\gamma_I - A_z\cos\omega\sin\omega_I$$

whereas $S_{z'}I_{y'}$ term is

$$- A_x\sin\omega\cos\gamma\sin\gamma_I + A_y\sin\omega\sin\gamma\cos\gamma_I$$

This term is zero when

$$\tan\gamma_I = (A_y/A_x)\tan\gamma = [(g_yA_y)/(g_xA_x)]\tan\phi$$

i.e., when

$$\sin\gamma_I = [g_y A_y / (g_x^2 A_x^2 \cos^2\phi + g_y^2 A_y^2 \sin^2\phi)^{1/2}] \sin\phi$$

$$\cos\gamma_I = [g_x A_x / (g_x^2 A_x^2 \cos^2\phi + g_y^2 A_y^2 \sin^2\phi)^{1/2}] \cos\phi$$

Then from $S_z, I_{x'}$ term we get

$$(A_x^2 \cos^2\gamma + A_y^2 \sin^2\gamma)^{1/2} \sin\omega\cos\omega_I - A_z \cos\omega\sin\omega_I = 0$$

which yields

$$\tan\omega_I = [(A_x^2 \cos^2\gamma + A_y^2 \sin^2\gamma)^{1/2} / A_z] \tan\omega$$
$$= [(g_x^2 A_x^2 \cos^2\phi + g_y^2 A_y^2 \sin^2\phi)^{1/2} / (g_z A_z)] \tan\alpha$$

The $S_z, I_{z'}$ term is then

$$A_x \sin\omega\cos\gamma\sin\omega_I\cos\gamma_I + A_y \sin\omega\sin\gamma\sin\omega_I\sin\gamma_I + A_z \cos\omega\cos\omega_I$$

$$= \frac{(g_x^2 A_x^2 \sin^2\alpha\cos^2\phi + g_y^2 A_y^2 \sin^2\alpha\sin^2\phi + g_z^2 A_z^2 \cos^2\alpha)^{1/2}}{(g_x^2 \sin^2\alpha\cos^2\phi + g_y^2 \sin^2\alpha\sin^2\phi + g_z^2 \cos^2\alpha)^{1/2}} = K$$

To get the second order terms, we must find $S_{x'}$ and $S_{y'}$ terms of $\underset{\sim}{S} \cdot \underset{\approx}{A} \cdot \underset{\sim}{I}$. The $S_{x'}, I_{z'}$ term becomes

$$A_x \cos\omega\cos\gamma\sin\omega_I\cos\gamma_I + A_y \cos\omega\sin\gamma\sin\omega_I\sin\gamma_I - A_z \sin\omega\cos\omega_I$$

which is equal to

$$\frac{g_\perp g_z}{g^2 K} (A_\perp^2 - A_z^2) \sin\alpha\cos\alpha$$

where $g_\perp = (g_x^2 \cos^2\phi + g_y^2 \sin^2\phi)^{1/2}$ and

$$A_\perp = (g_x^2 A_x^2 \cos^2\phi + g_y^2 A_y^2 \sin^2\phi)^{1/2} / g_\perp$$

The $S_{y'}, I_{z'}$ term becomes

$$- A_x \sin\gamma\sin\omega_I\cos\gamma_I + A_y \cos\gamma\sin\omega_I\sin\gamma_I$$

which is equal to

$$\frac{g_x g_y}{g_\perp g K} (A_y^2 - A_x^2) \sin\alpha\sin\phi\cos\phi$$

Also the $S_{x'}, I_{x'}$ term becomes

$$A_x \cos\omega \cos\gamma \cos\omega_I \cos\gamma_I + A_y \cos\omega \sin\gamma \cos\omega_I \sin\gamma_I + A_z \sin\omega \sin\omega_I$$

which is equal to

$$\frac{A_z A_\perp}{K}$$

Similarly

$$S_{y'} I_{x'} = - A_x \sin\gamma \cos\omega_I \cos\gamma_I + A_y \cos\gamma \cos\omega_I \sin\gamma_I$$

$$= \frac{g_x g_y g_z A_z}{g_\perp^2 g K A_\perp} (A_y^2 - A_x^2) \cos\alpha \sin\phi \cos\phi$$

$$S_{x'} I_{y'} = - A_x \cos\omega \cos\gamma \sin\gamma_I + A_y \cos\omega \sin\gamma \cos\gamma_I$$

$$= 0$$

$$S_{y'} I_{y'} = A_x \sin\gamma \sin\gamma_I + A_y \cos\gamma \cos\gamma_I$$

$$= A_x A_y / A_\perp$$

$$= g\beta H S_{z'} + K_{zz} S_{z'} I_{z'} + K_{xz} S_{x'} I_{z'} + K_{yz} S_{y'} I_{z'} + K_{xx} S_{x'} I_{x'}$$
$$+ K_{yx} S_{y'} I_{x'} + K_{yy} S_{y'} I_{y'}$$

where K_{xz} etc have been defined earlier. For the spin functions $M_S M_I$ the first order energies are

$$E = g\beta H M_S + K M_S M_I .$$

whereas the second order energy terms are found from

$$E = \sum_n \frac{< \psi_o | \hat{H}' | \psi_n > < \psi_n | \hat{H}' | \psi_o >}{E_o - E_n}$$

where the summation does not include n = 0.

For S = 1/2 consider the M_S = -1/2 state. We have carefully arranged so that there are no terms in the summation that include the S = 1/2 state. Therefore for M_S = -1/2 we get to second order:

$$E(-1/2, M_I) = -(1/2)g\beta H - (1/2)KM_I - \frac{(K_{xz}^2 + K_{yz}^2)}{4(g\beta H + KM_I)} M_I^2$$

$$- \frac{[(K_{xx} - K_{yy})^2 + K_{yz}^2]}{16[g\beta H + KM_I - (1/2)K]} [I(I + 1) - M_I(M_I + 1)]$$

$$\frac{[(K_{xx} + K_{yy})^2 + K_{yx}^2]}{16[g\beta H + KM_I - (1/2)K]} [I(I + 1) - M_I(M_I - 1)]$$

If we ignore KM_I and K compared to $g\beta H$, we get

$$E(-1/2, M_I) = -(1/2)g\beta H - (1/2)KM_I - \frac{K_{xx}K_{yy}}{4g\beta H} M_I$$

$$- \frac{(K_{xx}^2 + K_{yy}^2 + K_{yx}^2)}{8g\beta H} [I(I + 1) - M_I^2] - \frac{(K_{xz}^2 + K_{yz}^2)}{4g\beta H} M_I^2$$

Similarly

$$E(+1/2, M_I) = (1/2)g\beta H + (1/2)KM_I - \frac{K_{xx}K_{yy}}{4g\beta H} M_I$$

$$+ \frac{(K_{xx}^2 + K_{yy}^2 + K_{yx}^2)}{8g\beta H} [I(I + 1) - M_I^2] + \frac{(K_{xz}^2 + K_{yz}^2)}{4g\beta H} M_I^2$$

Therefore for $\Delta M_S = \pm 1$, $\Delta M_I = 0$ transition, we get

$$h\nu(M_I) = g\beta H + KM_I + \frac{(K_{xx}^2 + K_{yy}^2 + K_{yx}^2)}{4g\beta H} [I(I + 1) - M_I^2]$$

$$+ \frac{(K_{xz}^2 + K_{yz}^2)}{2g\beta H} M_I^2$$

where $K_{xx} = A_z A_\perp / K$; $K_{yy} = A_x A_y / A_\perp$;

$$K_{yx} = [(g_x g_y g_z A_z)/(g^2 g_\perp K A_\perp)] \times (A_y^2 - A_x^2) \cos\alpha \sin\phi \cos\phi$$

$$K_{xz} = [(gg_z)/(g^2 K)](A_\perp^2 - A_z^2) \sin\alpha \cos\alpha$$

$$K_{yz} = [(g_x g_y)/(g_\perp gK)](A_y^2 - A_x^2) \sin\alpha \sin\phi \cos\phi$$

For the MnO_4^{2-} system we will take the b-crystallographic direction to be the y direction. Then for the magnetic field along the b axis, $\alpha = 90°$, $\phi = 90°$, and hence

$K_{xx} = A_z A_y / A_y = A_z$; $K_{yy} = A_x A_y / A_y = A_x$; $K_{yx} = K_{yz} = 0$, and hence

$$h\nu(M_I) = g_y\beta H + A_y M_I + \frac{(A_z^2 + A_x^2)}{4g_y\beta H} [I(I + 1) - M_I^2]$$

or $$H(M_I) = \frac{h\nu_o}{g_y\beta} - \frac{A_y}{g_y\beta} - \frac{(A_z^2 + A_x^2)}{4g_y\beta h\nu_o} [I(I + 1) - M_I^2]$$

For two lines of similar $|M_I|$ values we have

$$(H_{M_I} + H_{-M_I})/2 = H^o - \frac{(A_z^2 + A_x^2)}{2g_y\beta h\nu_o} \{I(I + 1) - M_I^2\}$$

The last term in the above equation is estimated from the A_z, A_x and the first order values of g_y. H^o is then calculated from which g_y can be obtained.

For rotation in the xz plane $\phi = 0°$, so that

$K_{xx} = A_z A_x / K$ where $K = (g_x^2 A_x^2 \sin^2\alpha + g_z^2 A_z^2 \cos^2\alpha)^{1/2}/g$ and

$$g = (g_x^2\sin^2\alpha + g_z^2\cos^2\alpha)^{1/2}$$

Also $K_{yy} = A_x A_y / A_x = A_y$; $K_{yx} = 0 = K_{yz}$; and

$$K_{xz} = \frac{g_x g_z}{g^2 K} (A_x^2 - A_z^2)\sin\alpha\cos\alpha$$

Therefore

$$h\nu(M_I) = g\beta H + KM_I + \frac{(A_z^2 A_x^2 + A_y^2 K^2)}{4g\beta HK^2} [I(I + 1) - M_I^2]$$

$$+ \frac{g_x^2 g_z^2 (A_x^2 - A_z^2)^2}{2g^4 K^2 g\beta H} M_I^2\sin^2\alpha\cos^2\alpha$$

which on transposition gives

$$H(M_I) = \frac{h\nu_o}{g\beta} - \frac{KM_I}{g\beta} - \frac{(A_z^2 A_x^2 + A_y^2 K^2)}{4g\beta K^2 h\nu_o} [I(I+1) - M_I^2]$$

$$- \frac{g_x^2 g_z^2}{g^4} \frac{(A_x^2 - A_z^2)^2}{2K^2 g\beta h\nu_o} M_I^2 \sin^2\alpha \cos^2\alpha$$

For two lines of similar $|M_I|$ values the above equation becomes

$$\frac{(H_{M_I} + H_{-M_I})}{2} = H^o - \frac{(A_z^2 A_x^2 + A_y^2 K^2)}{2g\beta K^2 h\nu_o} \{I(I+1) - M_I^2\}$$

$$- \frac{g_x^2 g_z^2 (A_x^2 - A_z^2)^2}{g^5 K^2 \beta h\nu_o} M_I^2 \sin^2\alpha \cos^2\alpha$$

The last two terms are estimated with values of A_x, A_y, A_z and the first order values of g_x, g_y and g_z. H^o is calculated from which g can be obtained. The average value of g for each orientation was taken as the g value corrected for second order.

Near the maximum and minimum $\sin^2\alpha \cos^2\alpha = 0$ and we can use the same technique to calculate g that was used for the b-axis. In between, it is best to calculate the correction terms and α from the approximate values.

REFERENCES

1   E. Zavoisky, J. Phys. USSR, $\underline{9}$, 245 (1945); $\underline{10}$, 197 (1946)

2. A. Carrington, D. J. Ingram, K. A. K. Lott, D. S. Schonland and M. C. R. Symons, Proc. Roy. Soc.(london) A $\underline{254}$,101 (1956)

3. D. S. Schonland, Proc. Roy. Soc.(London) A $\underline{254}$, 111 (1956)

4. C. A. Kosky, B. R. McGarvey and S. L. Holt, J. Chem. Phys., $\underline{56}$, 5904 (1972)

5. E. Banks, M. Greenblatt and B. R. McGarvey, J.Chem. Phys., $\underline{47}$,33772 (1967)·

6. E. Banks, M. Greenblatt, B. R. McGarvey, J. Sol·d State Chem., $\underline{3}$,3308 (1971)

7. G. H. Azerbayejani and A. L. Merlo, Phys. Rev. A $\underline{137}$, 489 (1965)

8. A. D. Liehr and C. J. Ballhausen, Phys. Rev., $\underline{106}$, 1161 (1957)

9. J. M. Baker, B. Bleaney and K. D. Bowers, Proc. Roy. Soc. (London) B $\underline{69}$, 1205 (1956)

10. B. Bleaney and M. C. M. O'Br·en, Proc. Roy. Soc. (London) B $\underline{69}$, 1216 (1956)

11. I. A. Miller and E. L. Offenbacher, Phys. Rev., $\underline{166}$, 269 (1968)

12. S. A. Cotton and J. F. Gibson, J. Chem. Soc. A 803 (1971)

13. R. Richards, C. E. Johnson and H. A. O. H·ll, J. Chem. Phys., $\underline{53}$, 3118 (1970)

14. W. M. Reiff and R. E. DeS·mone, Inorg. Chem., $\underline{12}$, 1793 (1973)

15. R. E. DeSimone, J. Amer. Chem. Soc., $\underline{95}$, 6238 (1973)

16. J. H. M. Thornley, C. D. Lust·g and J. Owen, Proc. Roy. Soc. (London) C $\underline{1}$, 1024 (1956)

17. J. H. E. Griffiths, M. C. M. O'Brien, J. Owen, I. M. Ward and K. D. Bowers, Rep. Progr. Phys., _18_, 304 (1955)

18. H. S. Jarrett, J. Chem. Phys., _27_, 1298 (1957)

19. N. J. Hill, J. Chem. Soc., Faraday Trans., _11_, 427 (1972)

20. J. J. Fortman and R. G. Hayes, J. Chem. Phys., _43_, 15 (1965)

21. P. T. Manoharan and H. B. Gray, Chem. Commun., 324 (1965)

22. H. A. Kuska and M. T. Rogers, J. Chem. Phys., _42_, 3034 (1965)

23. B. R. McGarvey and J. Pearlman, J. Chem. Phys., _46_, 4992 (1967)

24. J. Owen and I. M. Ward, Phys. Rev., _102_, 591 (1956)

25. K. W. H. Stevens, Proc. Roy. Soc. (London) _C219_, 543 (1953)

26. H. Kon and N. E. Sharpless, J. Chem. Phys., _42_, 906 (1965)

27. K. DeArmond, B. B. Garrett and H. S. Gutowsky, J. Chem Phys., _42_, 1019 (1965)

28. B. R. McGarvey, J. Chem. Phys., _38_, 388 (1963)

29. B. B. Garrett, K. DeArmond ans H. S. Gutowsky, J. Chem. Phys., _44_, 3393 (1966)

30. B. R. McGarvey, Electron Spin Resonance of Metal Complexes, p. 1 , Plenum Press, 1969

31. C. W. F. T. Pistorius and M. C. Pistorius, Z. Krist., _117_, 259 (1962).

32. J. Sauka et al. LLatvijas Valsts. Univ. Zinatniske Rakst., _9_, 31 (1956)

33. A. W. Zacharieson and G. Zeigler, Z. Krisit., _8D_ 164 (1931)

34. K. Sahl, Beit. zur. Mineral. und Petrog. _9_, 111 (1963)

35. P. T. Manoharan and W. C. Hamilton, Inorg. Chem., _2_, 1043 (1963)

36. P. Wagner, B. S. Thesis, Polytechnic Institute of Brooklyn 1958

37. A. R. Patel and J. Koshy, J. Cryst. Growth, $\underline{2}$, 128 (1968)

38. G. Brauer, Handbook of Preparative Inorganic Chemistry,
     Translated By P. Stecher, Academic Press, New York, 1965

39. B. Bleaney, Phil. Mag., $\underline{42}$, 441 (1951)

40. E. Tepper, Ph.D. Thesis, Polytechnic Institute of Brooklyn,
     1968

41. M. Bailey and A. F. Wells, J. Chem. Soc., $\underline{217}$, 968(1961)

42. B. R. McGarvey, Private Communication

43. R. S. Mulliken, J. Chem. Phys., $\underline{23}$, 1833 (1958)

44. H. H. Jaffe, J. Chem. Phys., $\underline{21}$, 258 (1953)

45. H. H. Jaffe and G. O. Doak, J. Chem. Phys., $\underline{21}$, 196 (1953)

46. C. E. Moore, Atomic Energy Levels, National Bureau of
     Standards, Circular 467, Vol 1 (1949); Vol 2 (1952)

47. A. J. Freeman and R. E. Watson, Magnetism, Vol. 11A,
     Ed. G. J. Rado and H. Suhl, Academic Press, New York,
     1965, p. 167

48. E. Clementi and D. L. Raimondi, J. Chem. Phys.,
     $\underline{38}$, 2686 (1963)

49. B. R. McGarvey, J. Phys. Chem., $\underline{71}$, 51 (1967)

50. W. T. Oosterhuis, Moesbauer Eff. Methodol., $\underline{7}$, 97 (1971)

51. W. Haberditzl, K. D. Schleinitz and H. G. Bartel, Z.
     Naturforsch, B $\underline{24}$, 395 (1969)

52. B. N. Figgis, Introduction to Ligand Fields, J. W. Wiley,
     New York, 1966, p. 60

53. J. H. M. Thornley, J. Phys., $\underline{1}$, 1024 (1968)

54. S. A. Cotton, Inorg. Nucl. Chem. Lett., $\underline{8}$, 371 (1972)

55. H. A. Kuska and M. T. Rogers, J. Chem. Phys., $\underline{40}$, 910 (1964)

56   J. B. Morton, Chem. Rev., $\underline{64}$, 453 (1964)

57. E. F. G. Herington, T. Chem. Soc., 2747 (1956)

58. E. F. G. Herington, J. Chem. Soc., 4683 (1956)

59. B. R. McGarvey, J. Chem. Phys., $\underline{41}$, 3743 (1964)

60. D. Kivelson and S. Lee, J. Chem. Phys., $\underline{41}$, 1896 (1964)

61. A. Abragam, J. Horowitz and M. H. L. Pryce, Proc. Roy. Soc.)London), A $\underline{230}$, 169 (1955)

Date of Birth: August 15, 1938, Asaba, Nigeria.

Son of Obi Johnson Walter and Adaojei Ezzeh

Education: St. Patrick's College, Asaba, Nigeria,

1954-1960

University of Nigeria, Nsukka, Nigeria,

1961-1965, B.Sc.(Honours) Chemistry

Michigan State University, East Lansing,

Michigan, U.S.A.

1968, M.S., Physical Chemistry

University of Windsor, Windsor, Ontario, Canada,

1972-1974